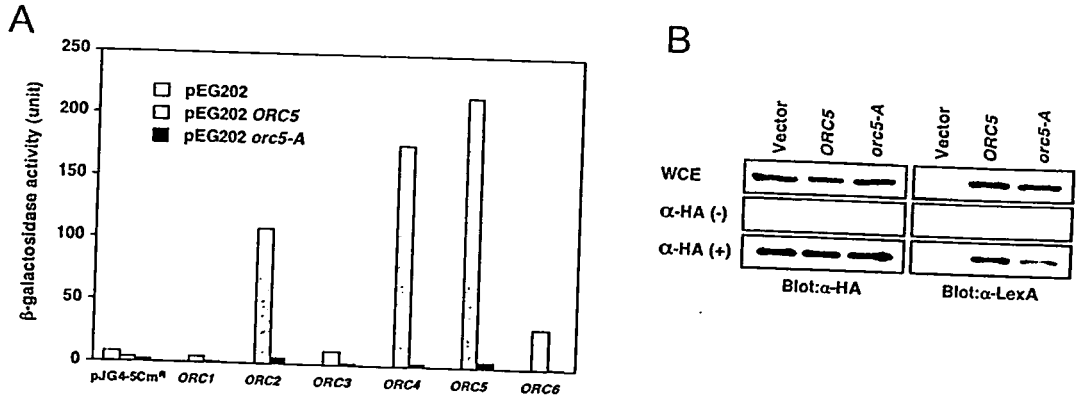

Figure 5 Interaction between Orc5p and Orc4p, and its dependency on the ATP-binding domain of Orc5p

(A) EGY48 cells were co-transfected with pSH18-34, a pEG202 derivative (pEG202 alone, or pEG202-*ORC5* or pEG202-*orc5-A*; BD fusions), and a pJG4-5Cm^R derivative (pJG4-5Cm^R alone, or pJG4-5Cm^R-*ORC1*, -*ORC2*, -*ORC3*, -*ORC4*, -*ORC5* or -*ORC6*; AD fusions). The activity of β-galactosidase in cells was determined and expressed as total units in 1 ml of yeast cell culture with D_{600} (attenuance) value as 1.0. (B) Whole cell extract was prepared from EGY48 cells having pSH18-34, pEG202 (vector) or its derivative (pEG202-*ORC5* or pEG202-*orc5-A*) and pJG4-5Cm^R-*ORC4* and precipitated with or without antibody against HA (Orc4p is tagged with HA in pJG4-5Cm^R-*ORC4*). Each sample [7.5% input of whole cell extract and precipitates with (+) or without (−) antibody against HA] was analysed on the same gel by immunoblotting with an antibody against HA or LexA.

interaction between Orc4p and Orc5p requires the ATP-binding domain of Orc5p.

For further confirmation that Orc5p's interaction with Orc4p depends on the ATP-binding domain of Orc5p, we examined colony formation on SC agar plates without leucine. Co-expression of BD-*ORC5* and AD-*ORC4* permitted colony formation, confirming that Orc4p and Orc5p interact (results not shown). Cells co-expressing BD-*orc5-A* and AD-*ORC4* fusions had only a weak ability to form colonies, especially at higher temperatures, suggesting that Orc5-Ap and Orc4p might interact weakly (results not shown). There was no clear difference between BD-*ORC5* and BD-*orc5-A* for colony formation on SC agar plates with leucine at any temperatures (results not shown). These results confirm that Orc4p interacts weakly with Orc5-Ap, compared with its interaction with Orc5p, especially at high temperatures. Since in ORC5-A (ORC containing the protein product of the *orc5-A* gene), Orc5p loses its ability to bind to ATP [12], ATP binding to Orc5p is presumably important for Orc5p and Orc4p to interact.

We then tried to determine the domain of each subunit (Orc5p and Orc4p) involved in the interaction. As shown in Figure 6(A), we created three fragments (N-terminal, middle and C-terminal) of Orc5p and Orc4p, constructed fusions, and examined the interaction between these fragments and an intact subunit. Co-expression of BD-*ORC5* and AD-*ORC4* caused a high level of β-galactosidase activity (Figure 6B). Co-expression of BD-N-terminal *ORC5* (termed *ORC51*) and AD-*ORC4* gave an even higher level of β-galactosidase activity. The other fragments of Orc5p seemed not to interact with Orc4p (Figure 6B). Co-expression of BD-*ORC4* and AD-*ORC5* caused the high level of β-galactosidase activity (Figure 6C). Co-expression of BD-C-terminal *ORC4* (termed *ORC43*) and AD-*ORC5* gave the lower but significant level of β-galactosidase activity (Figure 6C). The other fragments of Orc4p seemed not to interact with Orc5p. We confirmed that all fusion proteins were expressed approximately equally (results not shown). These results suggest that the N-terminal region of Orc5p interacts with the C-terminal region of Orc4p.

To test this idea, we examined the interaction between Orc43p and Orc51p using a yeast two-hybrid system. As shown in Figure 6(D), we could not detect the significant interaction between BD-*ORC43* and AD-*ORC51* or BD-*ORC51* and AD-*ORC43*. We confirmed that all fusion proteins were expressed approximately equally (results not shown). We consider a possibility that although the N-terminal region of Orc5p interacts with the C-terminal region of Orc4p, full-length of Orc5p and Orc4p are necessary to recognize the counterpart.

DISCUSSION

In the present study, we examined the mechanism of ORC disappearance from the *orc5-A* strain at high temperatures. Experiments with a chemical proteasome inhibitor, or with the *tan1-1* or *nob1-4* mutant, strongly suggested that ORC degradation is mediated by the proteasome system. At present, it is not clear whether Orc5p is the direct target of polyubiquitination, because we could not detect the polyubiquitination of Orc5-Ap in cells under our experimental conditions (results not shown). Observation that the introduction of the *tan1-1* mutation in the *orc5-A* mutant restored cell growth at high temperatures surprised us, because we considered that the growth defects were primarily due to a loss of function or structure of Orc5-A, and that elimination by the proteasome system was secondary to this. Precise identification of defects of the double mutant (*orc5-A*, *tan1-1*) is important in order to understand the role of ATP-binding to Orc5p in cells. Although we tried to find these, the mutant's colony formation ability at 37 °C, and cell viability after 37 °C incubation, were much the same as in wild-type cells.

FACS analysis revealed that in the *orc5-A* strain, at high temperatures, the cell cycle arrests at G_2/M. This arrest was also suppressed by *tan1-1*, suggesting that it is also due to ORC degradation by proteasomes. In human cells, one ORC subunit, Orc6p, plays an important role in chromosome segregation and cytokinesis. Orc6p localized to kinetochores during mitosis, and inhibition of Orc6p expression resulted in multi-polar spindles, aberrant mitosis and the formation of multinucleated cells [33]. Orc6p could also be required for chromosome segregation and cytokinesis in yeast, and this could explain why ORC degradation in the *orc5-A* mutant causes cell cycle arrest.

Analysis with a yeast two-hybrid system suggested that Orc5p preferentially interacts with Orc4p. These *in vivo* results are consistent with results from previous studies using other approaches *in vitro*. Lee and Bell reported, using protein-DNA cross-linking, that Orc4p and Orc5p are located very close to each other on

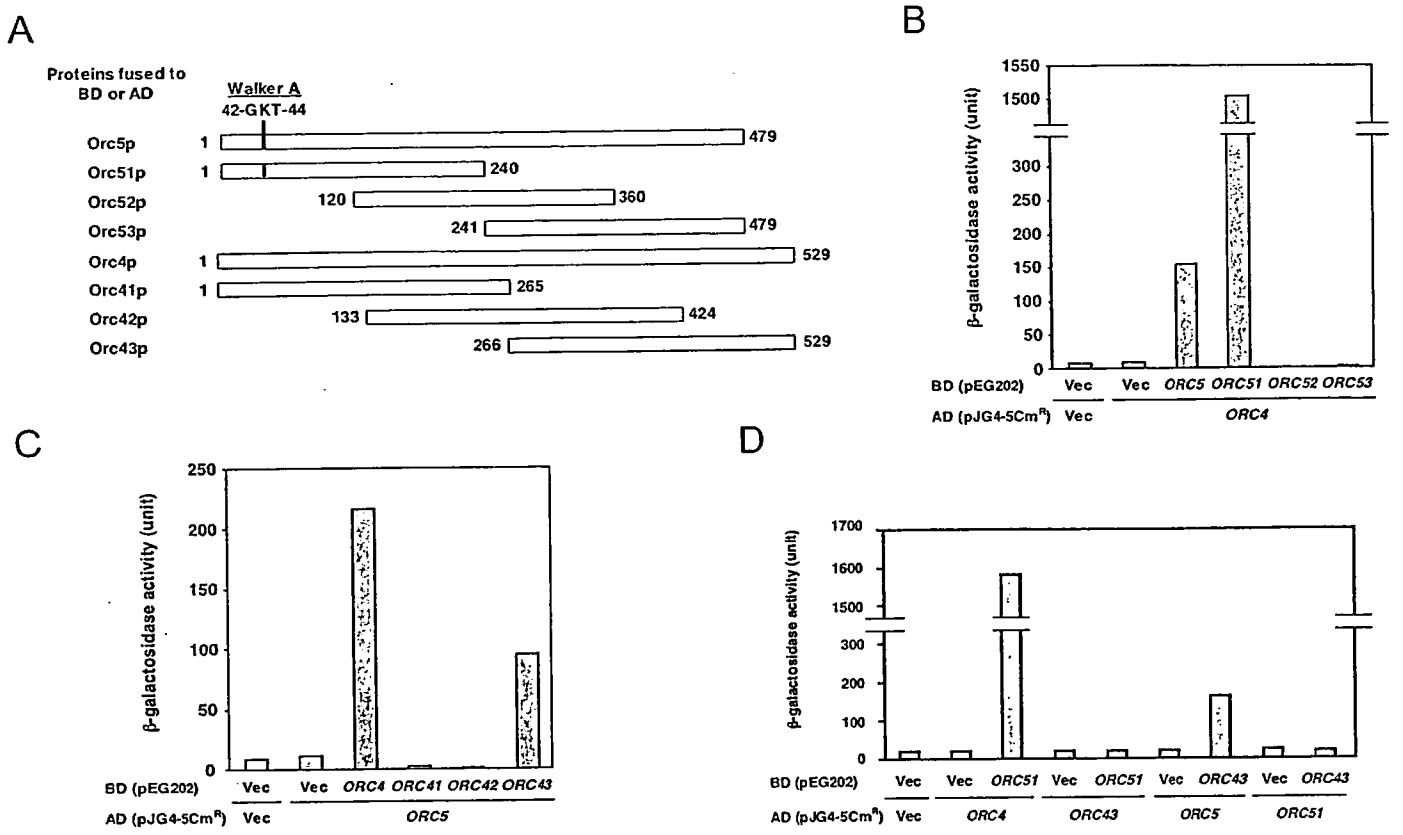

Figure 6 Mapping domains involved in the interaction between Orc5p and Orc4p, by using a yeast two-hybrid assay

Schematic diagram of Orc5p, Orc4p and their partial fragments (**A**). Amino acid residues of full-length Orc5p and Orc4p and their partial fragments were numbered (**A**). EGY48 cells co-transfected with pSH18-34, pJG4-5Cm^R derivatives and pEG202 derivatives. The activity of β-galactosidase in cells was expressed as described in the legend of Figure 5 (**B–D**).

origins of replication. They also showed that when ORC was purified from over-producing cells, lack of Orc5p led to a loss of Orc4p from purified ORC [34]. Therefore it seems that Orc4p and Orc5p interact both *in vitro* and *in vivo*. Kneissl et al. [35] studied the interaction between subunits of mouse ORC by use of a yeast two-hybrid system. The interaction between Orc4p and Orc5p was weak, compared with interactions between other subunits [35]. Thus the structure of ORC seems to be different in yeast and mouse. Analysis with a yeast two-hybrid system also suggested the Orc5p–Orc5p interaction and its dependence on ATP binding to Orc5p. We previously reported that ORC forms a multimer on origin DNA *in vitro* under the conditions of high concentrations of ORC [25]. It is an interesting idea that ORC forms a multimer *in vivo* under some conditions. Further *in vivo* analysis on the state of ORC at distinct phases of the cell cycle or under some environmental conditions is necessary to test this idea.

We suggest here, from use of the yeast two-hybrid system, that the interaction between Orc4p and Orc5p involves an ATP-binding site on Orc5p, and thus presumably depends on ATP bound to Orc5p; since purified Orc5p alone (without other subunits) does not bind ATP *in vitro*, we could not test the dependence of Orc4p–Orc5p interaction on ATP. In the *orc5-A* strain, both the defect in Orc4p–Orc5-Ap interaction, and enhanced ORC degradation, were apparent at high temperatures. Loss of the Orc4p–Orc5p interaction has probably led to the degradation of ORC. This idea is interesting because it is connected to another novel idea that ORC degradation is regulated by ATP binding to Orc5p even in wild-type cells. However, up to now, there is no reported evidence suggesting that wild-type ORC becomes unstable under some conditions. Furthermore, we previously reported that the ATP–Orc5p complex is relatively stable compared with the Orc1p–ATP complex [36]. Again, further analysis of the stability of wild-type ORC at distinct phases of the cell cycle or under some environmental conditions is necessary to test this idea.

We thank Dr Bruce Stillman (Cold Spring Harbor Laboratory, Cold Spring Harbor, U.S.A.) for providing antibodies against ORC, and Dr Kenji Kohno (Laboratory of Molecular and Cell Genetics, Nara Institute of Science and Technology, Nara, Japan) and Dr Akio Toh-E (Department of Biological Sciences, University of Tokyo, Tokyo, Japan) for providing yeast strains. The present study was supported by Grants-in-Aid for Scientific Research from the Ministry of Education, Culture, Sports, Science and Technology, Japan, by the Asahi Glass Foundation, by the Naito Foundation and by the Kato Memorial Foundation. M.M. and N.T. are Research Fellows of the Japan Society for the Promotion of Science.

REFERENCES

1 Sekimizu, K., Bramhill, D. and Kornberg, A. (1987) ATP activates DnaA protein in initiating replication of plasmids bearing the origin of the *E. coli* chromosome. Cell **50**, 259–265
2 Mizushima, T., Sasaki, S., Ohishi, H., Kobayashi, M., Katayama, T., Miki, T., Maeda, M. and Sekimizu, K. (1996) Molecular design of inhibitors of *in vitro* oriC DNA replication based on the potential to block the ATP binding of DnaA protein. J. Biol. Chem. **271**, 25178–25183
3 Mizushima, T., Takaki, T., Kubota, T., Tsuchiya, T., Miki, T., Katayama, T. and Sekimizu, K. (1998) Site-directed mutational analysis for the ATP binding of DnaA protein. Functions of two conserved amino acids (Lys-178 and Asp-235) located in the ATP-binding domain of DnaA protein *in vitro* and *in vivo*. J. Biol. Chem. **273**, 20847–20851
4 Katayama, T., Kubota, T., Kurokawa, K., Crooke, E. and Sekimizu, K. (1998) The initiator function of DnaA protein is negatively regulated by the sliding clamp of the *E. coli* chromosomal replicase. Cell **94**, 61–71

5 Mizushima, T., Nishida, S., Kurokawa, K., Katayama, T., Miki, T. and Sekimizu, K. (1997) Negative control of DNA replication by hydrolysis of ATP bound to DnaA protein, the initiator of chromosomal DNA replication in *Escherichia coli*. EMBO J. **16**, 3724–3730
6 Makise, M., Mima, S., Tsuchiya, T. and Mizushima, T. (2001) Molecular mechanism for functional interaction between DnaA protein and acidic phospholipids: identification of important amino acids. J. Biol. Chem. **276**, 7450–7456
7 Makise, M., Mima, S., Tsuchiya, T. and Mizushima, T. (2000) Identification of amino acids involved in the functional interaction between DnaA protein and acidic phospholipids. J. Biol. Chem. **275**, 4513–4518
8 Makise, M., Mima, S., Katsu, T., Tsuchiya, T. and Mizushima, T. (2002) Acidic phospholipids inhibit the DNA-binding activity of DnaA protein, the initiator of chromosomal DNA replication in *Escherichia coli*. Mol. Microbiol. **46**, 245–256
9 Sekimizu, K. and Kornberg, A. (1988) Cardiolipin activation of DnaA protein, the initiation protein of replication in *Escherichia coli*. J. Biol. Chem. **263**, 7131–7135
10 Xia, W. and Dowhan, W. (1995) *In vivo* evidence for the involvement of anionic phospholipids in initiation of DNA replication in *Escherichia coli*. Proc. Natl. Acad. Sci. U.S.A. **92**, 783–787
11 Bell, S. P. and Stillman, B. (1992) ATP-dependent recognition of eukaryotic origins of DNA replication by a multiprotein complex. Nature **357**, 128–134
12 Klemm, R. D., Austin, R. J. and Bell, S. P. (1997) Coordinate binding of ATP and origin DNA regulates the ATPase activity of the origin recognition complex. Cell **88**, 493–502
13 Takenaka, H., Makise, M., Kuwae, W., Takahashi, N., Tsuchiya, T. and Mizushima, T. (2004) ADP-binding to origin recognition complex of *Saccharomyces cerevisiae*. J. Mol. Biol. **340**, 29–37
14 Makise, M., Takenaka, H., Kuwae, W., Takahashi, N., Tsuchiya, T. and Mizushima, T. (2003) Kinetics of ATP-binding to origin recognition complex of *Saccharomyces cerevisiae*. J. Biol. Chem. **278**, 46440–46445
15 Dutta, A. and Bell, S. P. (1997) Initiation of DNA replication in eukaryotic cells. Annu. Rev. Cell Dev. Biol. **13**, 293–332
16 Takahashi, N., Yamaguchi, Y., Yamairi, F., Makise, M., Takenaka, H., Tsuchiya, T. and Mizushima, T. (2004) Analysis on origin recognition complex containing Orc5p with defective Walker A motif. J. Biol. Chem. **279**, 8469–8477
17 Kimata, Y., Higashio, H. and Kohno, K. (2000) Impaired proteasome function rescues thermosensitivity of yeast cells lacking the coatomer subunit epsilon-COP. J. Biol. Chem. **275**, 10655–10660
18 Estojak, J., Brent, R. and Golemis, E. A. (1995) Correlation of two-hybrid affinity data with *in vitro* measurements. Mol. Cell. Biol. **15**, 5820–5829
19 Thomas, B. J. and Rothstein, R. (1989) Elevated recombination rates in transcriptionally active DNA. Cell **56**, 619–630
20 Tone, Y. and Toh-E, A. (2002) Nob1p is required for biogenesis of the 26S proteasome and degraded upon its maturation in *Saccharomyces cerevisiae*. Genes Dev. **16**, 3142–3157
21 Scherer, S. and Davis, R. W. (1979) Replacement of chromosome segments with altered DNA sequences constructed *in vitro*. Proc. Natl. Acad. Sci. U.S.A. **76**, 4951–4955
22 Longtine, M. S., McKenzie, III, A., Demarini, D. J., Shah, N. G., Wach, A., Brachat, A., Philippsen, P. and Pringle, J. R. (1998) Additional modules for versatile and economical PCR-based gene deletion and modification in *Saccharomyces cerevisiae*. Yeast **14**, 953–961
23 Takahashi, N., Tsutsumi, S., Tsuchiya, T., Stillman, B. and Mizushima, T. (2002) Functions of sensor 1 and sensor 2 regions of *Saccharomyces cerevisiae* Cdc6p *in vivo* and *in vitro*. J. Biol. Chem. **277**, 16033–16040
24 Liang, C. and Stillman, B. (1997) Persistent initiation of DNA replication and chromatin-bound MCM proteins during the cell cycle in cdc6 mutants. Genes Dev. **11**, 3375–3386
25 Mizushima, T., Takahashi, N. and Stillman, B. (2000) Cdc6p modulates the structure and DNA binding activity of the origin recognition complex *in vitro*. Genes Dev. **14**, 1631–1641
26 Pickart, C. M. (2001) Ubiquitin enters the new millennium. Mol. Cell **8**, 499–504
27 Coux, O., Tanaka, K. and Goldberg, A. L. (1996) Structure and functions of the 20S and 26S proteasomes. Annu. Rev. Biochem. **65**, 801–847
28 Hershko, A. and Ciechanover, A. (1998) The ubiquitin system. Annu. Rev. Biochem. **67**, 425–479
29 Wilkinson, K. D. (1995) Roles of ubiquitinylation in proteolysis and cellular regulation. Annu. Rev. Nutr. **15**, 161–189
30 Saito, Y., Tsubuki, S., Ito, H. and Kawashima, S. (1990) The structure–function relationship between peptide aldehyde derivatives on initiation of neurite outgrowth in PC12h cells. Neurosci. Lett. **120**, 1–4
31 Jensen, T. J., Loo, M. A., Pind, S., Williams, D. B., Goldberg, A. L. and Riordan, J. R. (1995) Multiple proteolytic systems, including the proteasome, contribute to CFTR processing. Cell **83**, 129–135
32 Fields, S. and Song, O. (1989) A novel genetic system to detect protein–protein interactions. Nature **340**, 245–246
33 Prasanth, S. G., Prasanth, K. V. and Stillman, B. (2002) Orc6 involved in DNA replication, chromosome segregation, and cytokinesis. Science **297**, 1026–1031
34 Lee, D. G. and Bell, S. P. (1997) Architecture of the yeast origin recognition complex bound to origins of DNA replication. Mol. Cell. Biol. **17**, 7159–7168
35 Kneissl, M., Putter, V., Szalay, A. A. and Grummt, F. (2003) Interaction and assembly of murine pre-replicative complex proteins in yeast and mouse cells. J. Mol. Biol. **327**, 111–128
36 Makise, M., Takenaka, H., Kuwae, W., Takahashi, N., Tsuchiya, T. and Mizushima, T. (2003) Kinetics of ATP binding to the origin recognition complex of *Saccharomyces cerevisiae*. J. Biol. Chem. **278**, 46440–46445

Received 6 June 2006/9 November 2006; accepted 15 November 2006
Published as BJ Immediate Publication 15 November 2004, doi:10.1042/BJ20060841

BJ www.biochemj.org

Biochem. J. (2007) 402, 581–589 (Printed in Great Britain) doi:10.1042/BJ20061318

Endoplasmic reticulum chaperones inhibit the production of amyloid- peptides

Tatsuya HOSHINO*, Tadashi NAKAYA†, Wataru ARAKI‡, Keitarou SUZUKI*, Toshiharu SUZUKI† and Tohru MIZUSHIMA*[1]

*Graduate School of Medical and Pharmaceutical Sciences, Kumamoto University, Kumamoto 862-0973, Japan, †Graduate School of Pharmaceutical Sciences, Hokkaido University, Sapporo 060-0812, Japan, and ‡Department of Demyelinating Disease and Ageing, National Institute of Neuroscience, Kodaira 187-8502, Japan

A (amyloid- peptides) generated by proteolysis of APP (-amyloid precursor protein), play an important role in the pathogenesis of AD (Alzheimer's disease). ER (endoplasmic reticulum) chaperones, such as GRP78 (glucose-regulated protein 78), make a major contribution to protein quality control in the ER. In the present study, we examined the effect of overexpression of various ER chaperones on the production of A in cultured cells, which produce a mutant type of APP (APPsw). Overexpression of GRP78 or inhibition of its basal expression, decreased and increased respectively the level of A 40 and A 42 in conditioned medium. Co-expression of GRP78's co-chaperones ERdj3 or ERdj4 stimulated this inhibitory effect of GRP78. In the case of the other ER chaperones, overexpression of some (150 kDa oxygen-regulated protein and calnexin) but not others (GRP94 and calreticulin) suppressed the production of A . These results indicate that certain ER chaperones are effective suppressors of A production and that non-toxic inducers of ER chaperones may be therapeutically beneficial for AD treatment. GRP78 was co-immunoprecipitated with APP and overexpression of GRP78 inhibited the maturation of APP, suggesting that GRP78 binds directly to APP and inhibits its maturation, resulting in suppression of the proteolysis of APP. On the other hand, overproduction of APPsw or addition of synthetic A 42 caused up-regulation of the mRNA of various ER chaperones in cells. Furthermore, in the cortex and hippocampus of transgenic mice expressing APPsw, the mRNA of some ER chaperones was up-regulated in comparison with wild-type mice. We consider that this up-regulation is a cellular protective response against A .

Key words: amyloid- peptides (A), -amyloid precursor protein (APP), endoplasmic reticulum (ER) chaperone, glucose-regulated protein 78 (GRP78), protein maturation.

INTRODUCTION

AD (Alzheimer's disease) is the leading cause of adult onset dementia, with a dramatic increase in the incidence of AD apparent in our rapidly aging society. AD is pathologically characterized by the accumulation of tangles and senile plaques. Senile plaques are composed of the A (amyloid- peptides), A 40 and A 42 [1,2]. A is generated by secretase-dependent proteolysis of APP (-amyloid precursor protein). Prior to proteolysis, APP undergoes modification [for example, by N-glycosylation in the ER (endoplasmic reticulum) and *O*-glycosylation in the Golgi apparatus]. In order to generate A 40 and A 42, APP is first cleaved by -secretase and then by -secretase. For the cleavage of APP, -secretase competes with -secretase, which produces non-amyloidogenic peptides [3,4]. -Secretase is an aspartyl protease complex composed of four core components, including PS1 (presenilin 1) and PS2 [5]. The early onset familial form of AD (FAD) is linked to three genes, *APP*, *PS1* and *PS2* [5,6], strongly suggesting that the production of A is a key factor in the pathogenesis of AD. Therefore, cellular factors that suppress the generation of A provide important drug targets for the treatment of AD.

Proteins, including APP, first translocate into the ER where they undergo modification. N-glycosylation of APP in the ER is essential for the generation of A [4]. The ER is also proposed to be important for A -induced apoptosis of neuronal cells; for example, a potential intracellular target of A in mediating apoptosis, ERAB (ER-associated -binding protein), is an ER membrane protein [7,8]. Accumulation of unfolded protein in the ER induces the ER stress response, a process involving three types of ER transmembrane protein: IRE1 (protein-kinase and site-specific endoribonuclease), PERK (protein kinase R-like ER kinase) and ATF 6 (activating transcription factor 6) [9–11]. ER stressors phosphorylate PERK, which in turn phosphorylates eIF2 (eukaryotic initiation factor-2), leading to activation of ATF4 expression (ATF4 pathway) [12,13]. ER stressors also cause cleavage of $p90^{ATF6}$ into $p50^{ATF6}$, which translocates to the nucleus (ATF6 pathway) [11]. Both ATF4 and $p50^{ATF6}$ specifically activate transcription of ER stress response-related genes, including those genes that encode ER chaperones. A close relationship between the ER stress response and A has been suggested; mutations in the *PS1* or *PS2* genes increase cellular sensitivity to ER stressors by suppressing the activation of IRE1, PERK and ATF6 [14–18]. These observations suggest that the ER is an important cellular compartment for the pathogenesis of AD.

ER chaperones, such as GRP78 (glucose-regulated protein 78), GRP94, ORP150 (150 kDa oxygen-regulated protein), CRT (calreticulin) and CNX (calnexin), contribute greatly to protein quality control in the ER by assisting the refolding of unfolded proteins [19–21]. Therefore, it is reasonable to speculate that ER

Abbreviations used: A , amyloid- peptides; AD, Alzheimer's disease; AICD, -amyloid precursor protein intracellular domain; APP, -amyloid precursor protein; APPsw, Swedish mutant of APP; APPwt, wild-type APP; ATF6, activating transcription factor 6; CNX, calnexin; Co-IP, co-immunoprecipitation; CRT, calreticulin; CTF , C-terminal fragment ; DAPT, *N*-[*N*-(3,5-difluorophenacetyl-L-alanyl)]-S-phenylglycine *t*-butyl ester; DMEM, Dulbecco's modified Eagle's medium; EDEM, endoplasmic reticulum degradation-enhancing -mannosidase I-like protein; eIF2 , eukaryotic initiation factor-2 ; ER, endoplasmic reticulum; ERAD, ER-associated degradation; ERdj4 J, J domain-deleted ERdj4; FAD, familial AD; GRP, glucose-regulated protein; HEK-293, human embryonic kidney 293; HSP, heat shock protein; imAPP, immature APP; IRE1, protein-kinase and site-specific endoribonuclease; mAPP, mature APP; ORP150, 150 kDa oxygen-regulated protein; PERK, protein kinase R-like ER kinase; PS1, presenilin 1; RT, reverse transcriptase; sELISA, sandwich ELISA; siRNA, small interfering RNA.

[1] To whom correspondence should be addressed (email mizu@gpo.kumamoto-u.ac jp).

chaperones affect the generation of A and the pathogenesis of AD. In fact, some ER chaperones have been shown to physically interact with APP, and overexpression of GRP78 in cells decreases the level of both mature APP and secreted A [22,23]. Furthermore, the accumulation of GRP78 in senile plaques, the up-regulation of ER chaperones in the brains of AD patients and the co-localization of ER chaperones with A have all been reported [24–26]. In the present study, we systematically examined the effect of overexpression of various ER chaperones and found that some, but not all, suppress the generation of A *in vitro*. We propose that this suppression is due to inhibition of the secretase-dependent proteolytic processing of APP through direct interaction between ER chaperones and APP, resulting in the inhibition of APP maturation. Furthermore, we found that ER chaperones are up-regulated not only in cultured neuronal cells overproducing mutant forms of APP or treated with synthetic A 42, but also in the cortex and hippocampus of transgenic mice expressing mutant APP.

MATERIALS AND METHODS

Cell culture and overexpression of ER chaperones

HEK-293 (human embryonic kidney 293) or SH-SY5Y cells were cultured in DMEM (Dulbecco's modified Eagle's medium) or DMEM/Ham's-F12 medium respectively, supplemented with 10 % (v/v) fetal bovine serum, 100 units/ml penicillin and 100 g/ml streptomycin in a humidified atmosphere of 95 % air with 5 % CO_2 at 37 C. SH-SY5Y cells expressing APPsw (Swedish mutant of APP) or APPwt (wild-type APP) were described previously [27]. For transient expression of each gene, cells were seeded 24 h before the transfection in 24-well plates at a density of 1.5×10^5 cells/well. The transfection was carried out using Lipofectamine™ 2000 (Invitrogen) according to the manufacturer's instructions. Cells were used for experiments after a 24 h recovery period. Transfection efficiency was determined in parallel plates by transfection of the pEGFP-N1 control vector. Transfection efficiency was greater than 90 % in all experiments. The stable transfectants expressing each gene were selected by immunoblotting or real-time RT (reverse transcriptase)-PCR analyses. Positive clones were maintained in the presence of 800 g/ml G418, 100 g/ml zeocin or 200 g/ml hygromycin.

Immunoblotting analysis

Whole cell extracts were prepared as described previously [28]. For detection of CTF (C-terminal fragment) and CTF , membrane fractions were prepared as described previously [29]. The protein concentration of samples was determined by the Bio-Rad protein assay kit (Bio-Rad Laboratories), according to the manufacturer's instructions. Samples were applied to 7 % (for APP), 8 % (for GRP78), 10 % (for actin), 12 % (for His-tagged ERdj3), 15 % (for Myc-tagged ERdj4) or 16.5 % (for CTF and CTF ; v/v) polyacrylamide gels and subjected to SDS/PAGE, after which proteins were immunoblotted with respective antibodies.

sELISA (sandwich ELISA) assay for A

Cells were cultured for 24 h and the conditioned medium was subjected to sELISA using three types of specific monoclonal antibody, as described previously [30].

Co-IP (co-immunoprecipitation) assay

Co-IP was carried out as described previously [31], with some modifications. Cells were harvested, lysed with buffer (10 mM Hepes/KOH, pH 7.4, 150 mM NaCl and 0.5 % Triton X-100) and centrifuged at 20000 *g*. The antibody against the C-terminal fragment of APP was added to the supernatant, and the sample incubated for 12 h at 4 C with rotation. Dynabeads® coated with Protein A were then added and the samples were incubated for 2 h at 4 C and rotated, after which they were centrifuged at 20000 *g*. The beads were then washed four times with the same buffer and the proteins were eluted by boiling the beads in SDS sample buffer [62.5 mM Tris/Hcl, pH 6.8, 2 % (w/v) SDS, 5 % (v/v) 2-mercaptoethanol, 10 % (v/v) glycerol and 0.001 % Bromophenol Blue).

Real-time RT-PCR analysis

Total RNA was extracted from cells and mouse brain using an RNeasy kit according to the manufacturer's protocols (Qiagen). Samples were reverse-transcribed using a first-strand cDNA synthesis kit according to the manufacturer's instructions (Amershan Biosciences). Synthesized cDNA was subjected to real-time RT-PCR using SYBR® Green PCR Master Mix (Applied Biosystems) and analysed with ABI PRISM 7500 Sequence Detection software according to the manufacturer's instructions (Applied Biosystems). Real-time cycle conditions were 2 min at 50 C, followed by 10 min at 90 C and then 45 cycles at each of 95 C for 30 s and 63 C for 60 s. Specificity was confirmed by electrophoretic analysis of the reaction products and by inclusion of template- or RT-free controls. To normalize the amount of total RNA present in each reaction, the actin gene was used as an internal standard.

Statistical analysis

All values are expressed as the means _ S.D. Student's *t* test for unpaired results was used for the evaluation of differences between the two groups. Differences were considered to be significant for P 0.05.

RESULTS

ER chaperones inhibit the generation of A

We based our investigations on HEK-293 cells that stably express APP with the double mutations, K651N/M652L, known as the 'Swedish' mutations (APPsw) [30]. These mutations elevate cellular and secreted levels of A [32]. The effect of ER chaperones on the generation of A 40 and A 42 was monitored by determining the amount of these peptides in conditioned medium by sELISA after transient transfection of the cells with expression plasmid for each ER chaperone. Transient overexpression of GRP78 (Figure 1A) caused a decrease in the level of A 40 and A 42 (Figures 1B and 1C) suggesting that GRP78 inhibits the production of A . This was confirmed using siRNA (small interfering RNA). Transfection of siRNA against GRP78 not only caused a decrease in the background cellular expression of GRP78 (Figure 1D), but also led to a weak increase in the level of A 40 and A 42 in the conditioned medium (Figures 1E and 1F). The weakness of the induction may be due to other ER chaperones compensating for the function of GRP78 under the experimental conditions (see Supplementary Figure S2 at http://www.BiochemJ.org/bj/402/bj4020581add.htm).

GRP78 belongs to the HSP70 (heat shock protein 70) family of proteins for which co-chaperones have also been identified [19]. For example, HSP40 binds to HSP70, stimulating its ATPase and chaperone activities [33]. Various co-chaperones have been suggested for GRP78, among which ERdj3 and ERdj4 have been

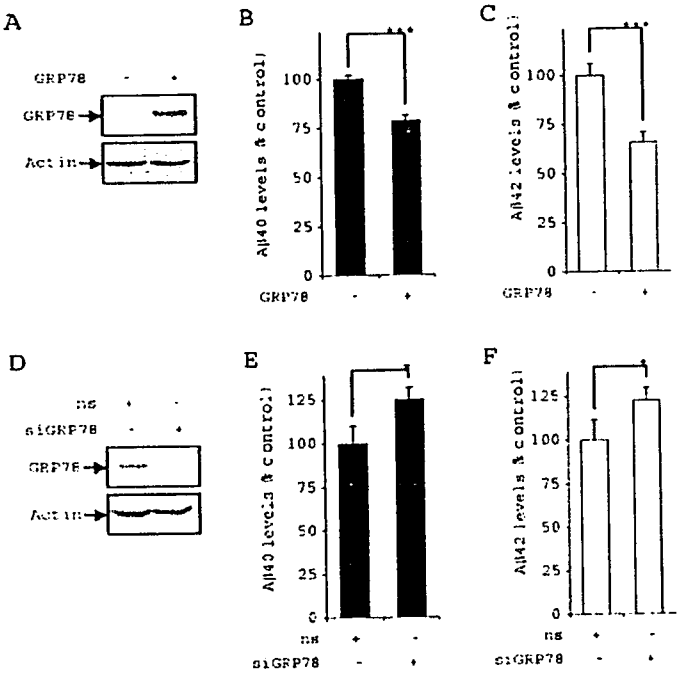

Figure 1 Inhibition of A generation by transient expression of GRP78

HEK-293 cells expressing APPsw were transiently transfected either with expression plasmid for GRP78 or control vector (**A–C**), or with siRNA against GRP78 (siGRP78) or non-silencing (ns) siRNA (**D–F**), after which they were cultured for 24 h. Whole cell extracts (10 g protein) were analysed by immunoblotting with an antibody against GRP78 (**A**) or actin (**D**). To detect GRP78 in the control sample, a relatively longer exposure was used in (**D**) than in (**A**). The amount of A 40 and A 42 in the conditioned medium was determined by sELISA and expressed relative to the control. Results are means _ S.D. (n 3). ***, P 0.001; *, P 0.05 (**B**, **C**, **E** and **F**).

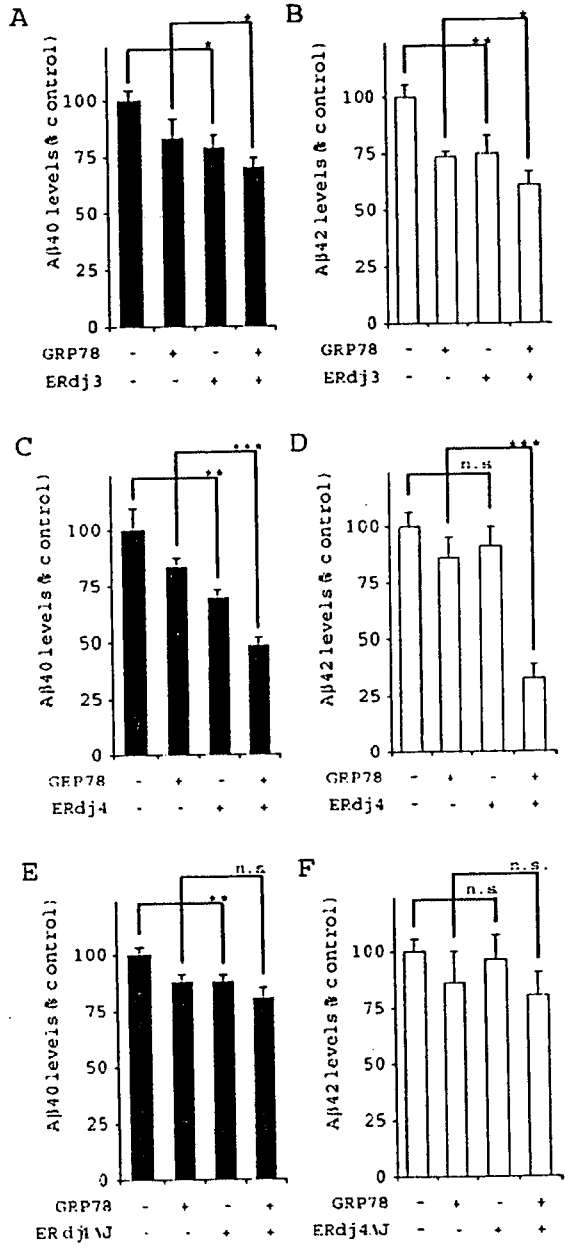

Figure 2 Stimulation by ERdj3 or ERdj4 of inhibitory effect of GRP78 on A generation

HEK-293 cells expressing APPsw were transiently transfected with expression plasmid for GRP78 (**A–F**), ERdj3 (**A** and **B**), ERdj4 (**C** and **D**), ERdj4 J (**E** and **F**) and/or control vector (**A–F**), with total DNA amounts fixed at 1 g, and cultured for 24 h. The amount of A 40 and A 42 in the conditioned medium was determined and expressed as described in the legend for Figure 1. Results are means _ S.D. (n 3). ***, P 0.001; **, P 0.01; *, P 0.05. n.s., not significant.

shown to bind to GRP78, enhancing its ATPase and chaperone activities [34,35]. Here we examined the effect of overexpression of ERdj3 and ERdj4, or their co-expression with GRP78, on A generation. Overexpression of ERdj3 or ERdj4 was confirmed by immunoblotting (see Supplementary Figure S1 at http://www.BiochemJ.org/bj/402/bj402058 1add.htm) and real-time RT-PCR (results not shown) and found that the level of overexpression of GRP78 (or ERdj3 and ERdj4) was not affected by simultaneous overexpression of ERdj3 and ERdj4 (or GRP78; see Supplementary Figure S1). As illustrated in Figures 2(A) and 2(B), transfection of an expression plasmid for ERdj3 decreased the level of both A 40 and A 42. Furthermore, co-transfection of expression plasmids for both GRP78 and ERdj3 produced an even greater decrease (Figures 2A and 2B). Although the transfection of an expression plasmid for ERdj4 significantly decreased the level of A 40 but not A 42 (Figures 2C and 2D), co-transfection of expression plasmids for both GRP78 and ERdj4 caused a clear decrease in both peptides; co-overexpression of both GRP78 and ERdj4 decreased the level of A 42 to about 30% of the control level (Figure 2D). These results show that ERdj3 and ERdj4 stimulate the inhibitory effect of GRP78 on the generation of A and suggest that this effect of GRP78 involves its ATPase and chaperone activities. The slight inhibitory effect of overexpression of ERdj3 or ERdj4 alone on the generation of A may be due to the activation of endogenous GRP78 by these co-chaperones.

The J domain of the HSP40 family of proteins is responsible for their interaction with the HSP70 family of proteins [33]. It has been shown that the J domain of ERdj4 is essential for its interaction with GRP78 [35]. As shown in Figures 2(E) and 2(F), and in comparison with the results obtained with the wild-type ERdj4 (Figures 2C and 2D), transfection of an expression plasmid for ERdj4 J (J domain-deleted ERdj4) had less activity in the stimulation of the effect of GRP78 on A generation. A similar level of overexpression between wild-type ERdj4 and ERdj4 J was confirmed by immunoblotting (see Supplementary Figure S1) and real-time RT-PCR (results not shown). These findings suggest that the inhibitory effect of ERdj4 (and maybe ERdj3) on A production seems to be achieved via its interaction with GRP78.

We also examined the effect of ER chaperones other than GRP78 (ORP150, GRP94, CNX and CRT). Overexpression of

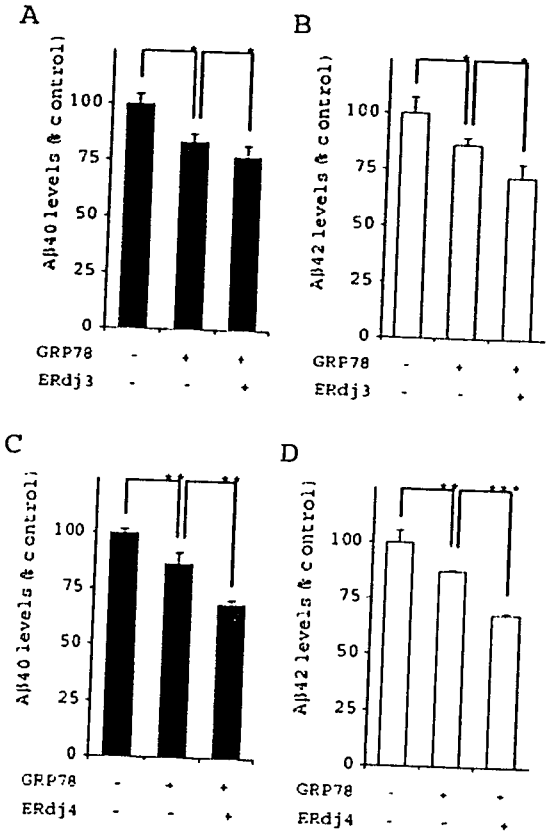

Figure 3 Inhibition of A generation in clones stably expressing ER chaperones

HEK-293 clones expressing APPsw and the indicated ER chaperones were cultured for 24 h. The amount of A 40 and A 42 in the conditioned medium was determined and expressed as described in the legend for Figure 1. Results are means _ S.D. (n 3). ***, P 0.001; **, P 0.01; *, P 0.05.

each ER chaperone was confirmed by immunoblotting and/or real-time RT-PCR analyses (results not shown). The results revealed that these ER chaperones can be classified into three groups. As well as GRP78, overexpression of ORP150 decreased the level of both A 40 and A 42. Overexpression of CNX decreased the level of A 42 but not that of A 40. On the other hand, the expression of GRP94 and CRT had no effect on the level of either A 40 or A 42 (see Supplementary Figure S2). Thus, while the suppression of A production is not specific to GRP78, neither is it a general feature of all ER chaperones.

Mechanism for inhibitory effect of GRP78 on A generation

In order to examine the molecular mechanism governing the inhibitory effect of GRP78 on A production, we produced HEK-293 cells that stably expressed not only APPsw, but also GRP78, His-tagged ERdj3 and/or Myc-tagged ERdj4. Expression of each ER chaperone was confirmed by immunoblotting (which are shown in Figures 5A and 5C). First, we examined the production of A in each clone. As shown in Figure 3, the level of both A 40 and A 42 in the conditioned medium was decreased for the GRP78-overexpressing clone. A further decrease was observed for clones overexpressing GRP78 and ERdj3 or ERdj4, which was consistent with the results obtained from our transient-expression experiments (Figure 2). However, the difference in the effects of ERdj4 and ERdj3, as illustrated in Figure 2, was not observed in stable-expression experiments (Figure 3).

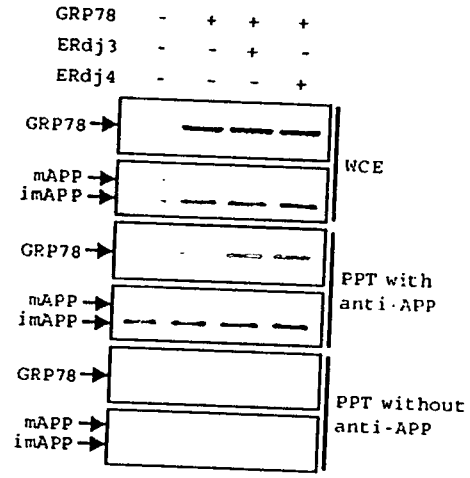

Figure 4 Co-IP of GRP78 with APP

Whole cell extracts prepared from HEK-293 clones expressing APPsw and the indicated ER chaperones were precipitated with or without antibody against the CTF of APP. Whole cell extracts (WCE) and the precipitates (PPT) with or without the antibody were analysed by immunoblotting with antibodies against GRP78 or APP.

Using these clones, the physical interaction of GRP78 with APP was estimated by co-IP. The mature (N- and *O*-glycosylated) and immature (N-glycosylated alone) forms of APP (mAPP and imAPP respectively) can be separated by SDS/PAGE on the basis of their molecular masses [36]. As shown in Figure 4, GRP78 was co-precipitated with APP in a manner that was dependent on the antibody against APP, which showed that GRP78 physically interacted with APP. Furthermore, co-expression of either ERdj3 or ERdj4 slightly stimulated this interaction (Figure 4).

We then examined the maturation of APP, an essential step in the production of A that ocuured in ER. As shown in Figures 5(A) and 5(B), the amount of mAPP relative to imAPP was decreased in the GRP78-overexpressing clone, with a further decrease being observed in the clone expressing both GRP78 and ERdj3. Similar results were obtained with ERdj4 (Figures 5C and 5D). These results suggest that GRP78 inhibits the maturation of APP and that this action is stimulated by its co-chaperones.

We also performed pulse-chase labelling experiments. Proteins were pulse-labelled with [^{35}S]methionine, chased with excess amounts of cold methionine, precipitated with antibody against APP and then examined by autoradiography. Compared with the controls, the conversion of labelled imAPP to mAPP and the disappearance of labelled imAPP and mAPP were retarded in clones expressing GRP78/ERdj3 or GRP78/ERdj4 (see Supplementary Figure S3 at http://www.BiochemJ.org/bj/402/bj4020581add.htm). These results show that the maturation of APP was inhibited, whereas the half-life of APP was prolonged, by the overexpression of GRP78/ERdj3 or GRP78/ERdj4.

Based on the results described above, we speculated that the inhibition of A production by ER chaperones is due to the inhibition of secretase-dependent APP proteolysis as a result of inhibition of APP maturation. In order to assess this, we attempted to detect the CTFs of APP that are generated by -, - and -secretase (CTF , CTF and CTF respectively). CTF could not be detected using our experimental conditions (results not shown). However, as shown in Figure 6, the amount of CTF and CTF was decreased in the GRP78-overexpressing clone, with a further decrease being observed in clones overexpressing GRP78/ERdj3 or GRP78/ERdj4. Based on these results we consider that proteolysis of APP by - and -secretases is inhibited in cells overexpressing these ER chaperones.

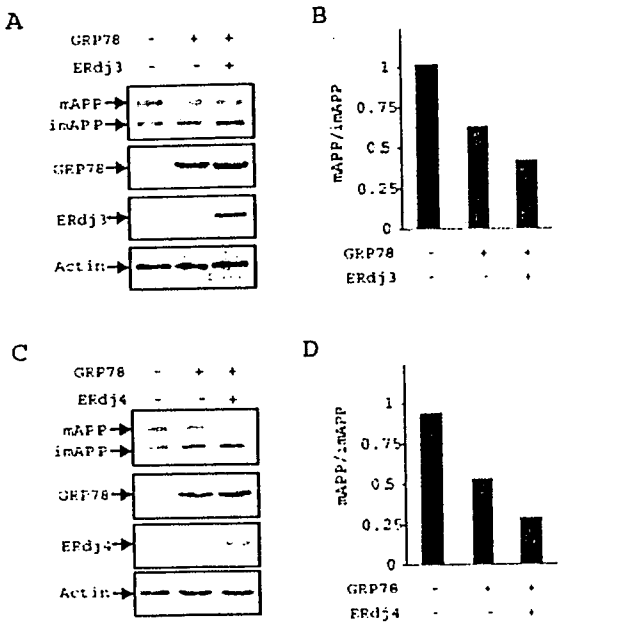

Figure 5 Effect of ER chaperones on the maturation of APP

HEK-293 clones expressing APPsw and the indicated ER chaperones were cultured for 24 h. Whole cell extracts (10 g protein) were analysed by immunoblotting with antibodies against GRP78, the CTF of APP, the His-tag (for ERdj3), the Myc-tag (for ERdj4) and actin (**A** and **C**). The band intensity ratio (mAPP/imAPP) was determined (**B** and **D**). Similar results were obtained in independent experiments.

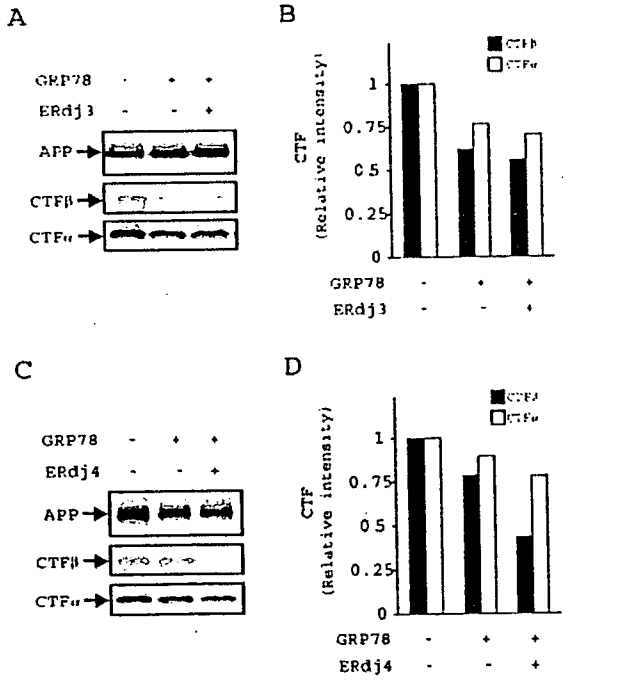

Figure 6 Effect of ER chaperones on the amount of CTF and CTF in cells

HEK-293 clones expressing APPsw and the indicated ER chaperones were cultured for 24 h. Membrane fractions (20 g protein) were analysed by immunoblotting with antibodies against APP and the CTF and CTF of APP in response to GRP78 and ERdj3 (**A**) or ERdj4 (**C**). The band intensity was determined and expressed relative to the control (**B** and **D**). Similar results were obtained in independent experiments.

Unfolded or misfolded proteins in the ER are degraded by a system, called ERAD (ER associated degradation), which is mediated by the proteasome system [9]. Therefore, it is possible that ERAD is involved in the inhibitory effect of GRP78 on A production. To address this issue, we examined the effect of a proteasome inhibitor (lactacystin) on A production. As shown in Supplementary Figure S4 (http://www.BiochemJ.org/bj/402/bj4020581add.htm), lactacystin did not affect the level of A production in either the presence or absence of GRP78-overexpression, excluding a possibility described above.

Up-regulation of mRNA of ER chaperones by A

It is well known that A is toxic to neuronal cells both *in vitro* and *in vivo*, and this toxicity seems to play an important role in the pathogenesis of AD [37]. The results described above suggest that ER chaperones protect cells against A by decreasing the amount of secreted A . Therefore, it is reasonable to speculate that cells up-regulate ER chaperones in response to A in order to protect themselves. To test this idea, we first compared the mRNA expression of various ER chaperones between APPsw-overexpressing, APPwt-overexpressing and control neuroblastoma (SH-SY5Y) cells [27]. As shown in Figure 7(A), the mRNAs of all of the ER chaperones tested were up-regulated in APPsw-overexpressing cells but not in APPwt-overexpressing cells. We also showed that GRP78 was weakly induced by overexpression of APPsw but not APPwt (see Supplementary Figure S5 at http://www.BiochemJ.org/bj/402/bj4020581add.htm). An inhibitor of -secretase, DAPT {*N*-[*N*-(3,5-difluorophenacetyl-L-alanyl)]-S-phenylglycine *t*-butyl ester}, attenuated this up-regulation (Figure 7A), strongly suggesting that -secretase-dependent proteolytic fragments of APP (such as A), but not APP itself, are responsible for this upregulation. As shown in Figure 7(B), the level of A in the culture medium was much higher in APPsw-overexpressing cells than APPwt-overexpressing cells, and treatment of cells with DAPT caused the decrease in the level of A . We therefore examined the effect of adding synthetic A 42 to the conditioned medium on mRNA expression of various ER chaperones (Figure 7C). In all cases there was a dose-dependent upregulation of the ER chaperone mRNA. A 42 at a concentration of 0.1 M or 1 M did not affect the cell viability; however, treatment of cells for 48 h with 10 M A 42 caused apoptosis in 5–10% of the cells (results not shown).

Both the ATF4 and ATF6 pathways are involved in the up-regulation of ER chaperones by ER stressors [11–13]. In the present study, we used siRNAs against ATF4 and ATF6 to examine the contribution of these transcription factors to A 42-dependent up-regulation of ER chaperones. As shown in Figures 8(A) and 8(B), transfection of a given siRNA suppressed the expression of its target gene, but not the other gene, regardless of the presence or absence of A 42. A 42-dependent up-regulation of *GRP78* mRNA was partially suppressed by siRNA against either ATF4 or ATF6 (Figure 8C). Similar results were obtained for A 42-dependent up-regulation of mRNA of other ER chaperones (Figures 8D–8I). None of the transfections illustrated in Figure 8 affected the baseline cell viability (results not shown). These results suggest that both the ATF4 and ATF6 pathways are involved in the up-regulation of ER chaperones by A 42.

In order to test the *in vivo* relevance of the upregulation of ER chaperones by expression of APPsw in neuronal cells, we compared the mRNA expression of various ER chaperones in the brains (cortex and hippocampus) of transgenic mice expressing APPsw (APP23) and wild-type mice. The cortex and hippocampus were chosen for investigation as these are the main areas involved in senile plaque formation [38,39]. As shown in Figure 9,

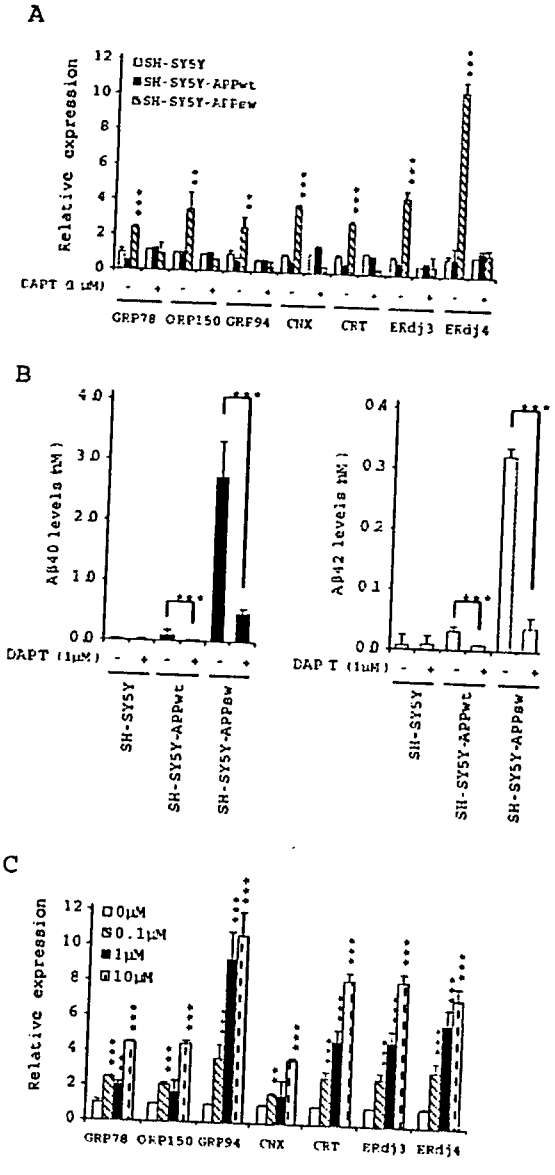

Figure 7 Up-regulation of mRNA of various ER chaperones by expression of APPsw or addition of synthetic A 42

SH-SY5Y clones expressing APPwt, APPsw and vector control were cultured for 48 h in the presence or absence of 1 M DAPT (**A** and **B**). SH-SY5Y cells were cultured for 48 h in the presence of the indicated concentrations of A 42 (**C**). Total RNA was extracted and subjected to real-time RT-PCR using specific primers for each chaperone. Values were normalized to actin gene expression and expressed relative to the control (**A** and **C**). The amount of A 40 and A 42 in the conditioned medium was determined and expressed as described in the legend for Figure 1(B). Results are means _ S.D. (*n* 3). ***, *P* 0.001; **, *P* 0.01.

the mRNA level of some, but not all, of the tested ER chaperones were significantly up-regulated in APP23 mice (at 6-months old) compared with wild-type controls. The increase in the amount of A and development of senile plaques were reported in APP23 mice of this age [40]. Among the ER chaperones, both GRP78 and ORP150 were significantly up-regulated at the mRNA level in both the cortex and hippocampus of APP23 mice (Figure 9). These findings suggest that the *in vitro* results obtained in the present study are functionally significant, reflecting the *in vivo* relevance of our cell culture studies.

DISCUSSION

In the present study, we have shown that, consistent with previous results [22], overexpression of GRP78 in cells decreases the amount of A 40 and A 42 in conditioned medium. Furthermore, we found that some, but not all, of the ER chaperones have a similar activity. Expression of ORP150 decreased the level of both A 40 and A 42 more significantly than GRP78, whereas expression of CNX decreased the level of A 42 alone; neither CRT nor GRP94 had any effect. At present, it is unclear what underlies these differences. Given that CNX and CRT have similar biochemical activities and are thought to play similar roles in cells [21], their differing effect on A 42 production is of particular interest. One possibility is that their different cellular locations are responsible for their differing effects. Similar to APP, CNX locates in the ER membrane, whereas CRT is an ER-soluble protein [21]. This difference in location is believed to underlie the differing contributions of these proteins to ERAD; CNX, but not CRT, binds to EDEM (ER degradation-enhancing -mannosidase I-like protein; an important protein for ERAD), resulting in the stimulation of ERAD [41].

In order to uncover the mechanism responsible for the decrease in the level of secreted A following overexpression of ER chaperones, we performed several experiments. Since the level of CTF and CTF also decreased in cells expressing ER chaperones, the decrease in the level of secreted A seems to be due to inhibition of secretase-dependent proteolytic processing of APP. Co-expression of ERdj3 or ERdj4 but not ERdj4 J stimulated the GRP78-dependent inhibition of A production. We also showed that GRP78 was co-immunoprecipitated with APP. Furthermore, overexpression of GRP78/ERdj3 or GRP78/ERdj4 inhibited the maturation of APP in cells. These results suggest that GRP78 binds directly to APP, inhibiting its maturation, which results in the suppression of secretase-dependent proteolytic processing of APP. We consider that the interaction of GRP78 with APP inhibits the translocation of APP from the ER to the Golgi apparatus, where maturation of APP is completed [4].

We also found that overproduction of APPsw in cells causes up-regulation of the mRNAs of various ER chaperones. Given that this upregulation is diminished by treatment of cells with an inhibitor of -secretase (DAPT), and that addition of synthetic A 42 to the conditioned medium also caused upregulation of the mRNA of various ER chaperones, A but not APP itself seems to be responsible for this up-regulation. However, in experiments designed to examine the effect of overproduction of APPsw in cells, the concentration of A 42 in the conditioned medium was about 0.3 nM, this being much lower than the concentration of synthetic A 42 required for up-regulation of ER chaperones (about 100 nM). There are three possibilities to explain this discrepancy: (i) endogenous A 42 is more active than the synthetic form in terms of up-regulating ER chaperones; (ii) endogenous A 42 acts in cells before being secreted into the conditioned medium; and (iii) although a previous study has shown that A 42 is more neurotoxic than A 40 [42], it is possible that A 40 but not A 42 is responsible for the up-regulation of ER chaperones. Another potential discrepancy lies in the findings of Kadowaki et al. [43], who reported that A 42 (up to 40 M) did not up-regulate GRP78 in PC12 cells, based on immunoblotting and RT-PCR (not real-time RT-PCR) experiments. However, this difference may be due to variations in the cell types and experimental methods used.

In terms of the mechanism underlying the up-regulation of ER chaperones by A , we found that siRNA against either ATF4 or ATF6 partially suppressed this effect, indicating the involvement of both the PERK/eIF2 /ATF4 and ATF6 pathways. Another ER transmembrane protein, IRE1, may also be involved. However,

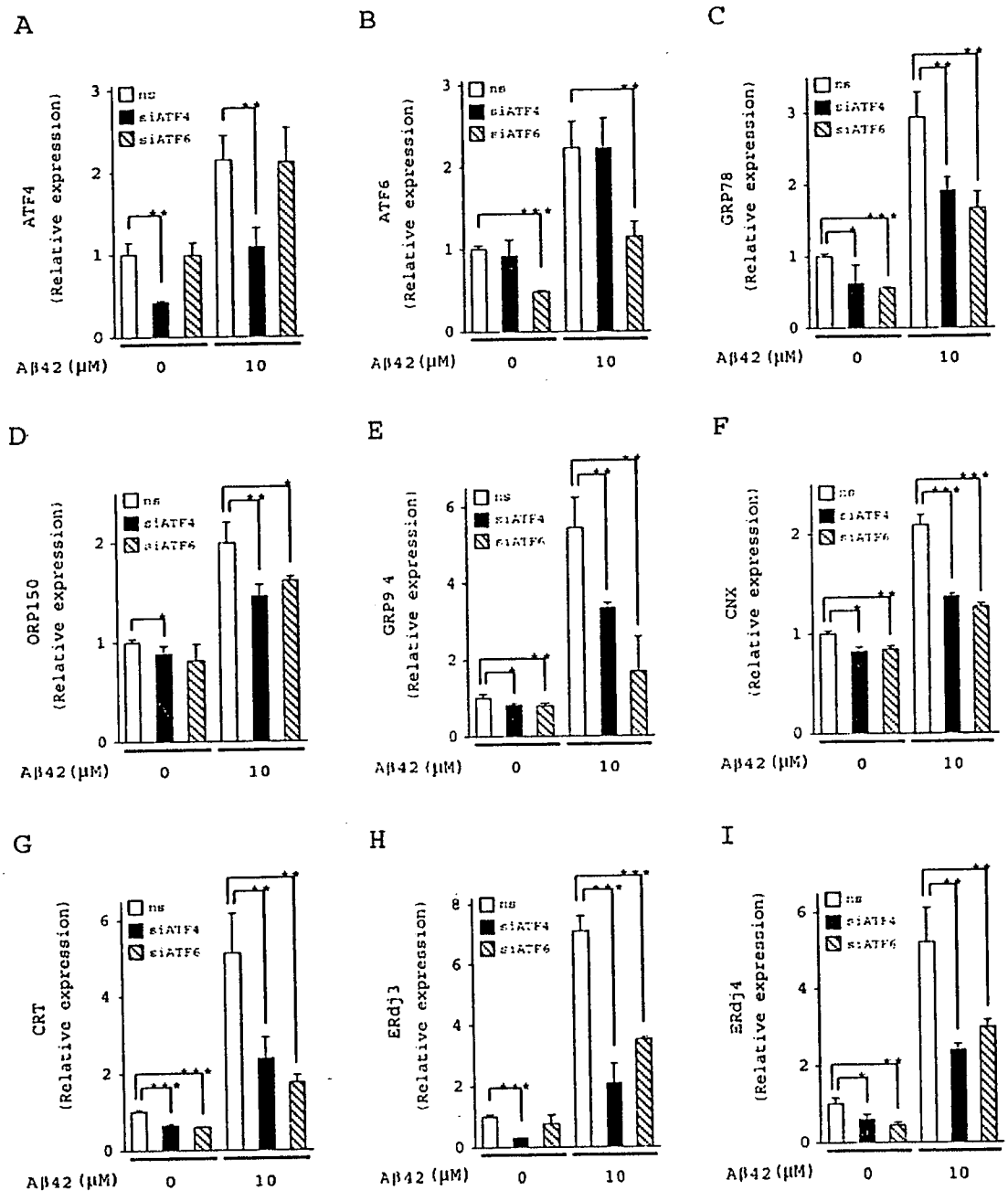

Figure 8 Effect of siRNA for ATF4 or ATF6 on the A 42-dependent up-regulation of ER chaperone mRNA

SH-SY5Y cells transfected with siRNA against ATF4 (siATF4), ATF6 (siATF6) and/or non-silencing (ns) siRNA (the total amount of siRNA was fixed at 5 g) were incubated with or without 10 M A 42 for 48 h. Total RNA was extracted and subjected to real-time RT-PCR by use of specific primers for each gene. Values were analysed and expressed as described in the legend for Figure 7(A). Results are means _ S.D. (n 3). ***, P 0.001; **, P 0.01; *, P 0.05.

since none of the siRNAs against IRE1 that were tested in the present study significantly suppressed the target gene (results not shown), we could not test the contribution of the IRE1-pathway to A 42-dependent up-regulation of ER chaperones. In considering the mechanism upstream of activation of ER transmembrane proteins by A , we believe that an increase in intracellular Ca^2 plays an important role. It is well known that changes in cellular Ca^2 levels can induce the ER stress response [44,45]. It has also been reported that addition of A to neuronal cells leads to a rise in the concentration of intracellular Ca^2 by stimulating the influx of extracellular Ca^2 and efflux of ER Ca^2 [46,47]. It was found recently that AICD (APP intracellular domain) stimulates the transcription of some genes [48]. Therefore, it is also possible that AICD is involved in the up-regulation of ER chaperones by A .

In the cortex and hippocampus of transgenic mice expressing APPsw, some ER chaperones were also up-regulated, suggesting that A exerts an effect both *in vitro* and *in vivo*. It is therefore possible that this *in vivo* up-regulation contributes to the protection of neurons by inhibiting the production of A , which was also observed *in vitro*. Furthermore, as described above, the accumulation of GRP78 in senile plaques, the up-regulation of ER chaperones in the brain of AD patients and the co-localization of ER chaperones and A have all been reported [24,25], highlighting

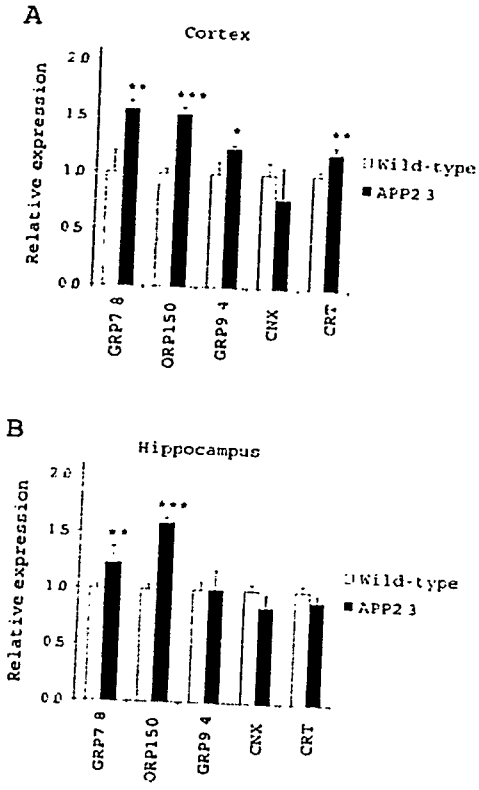

Figure 9 Expression of mRNA of various ER chaperones in cortex and hippocampus in transgenic mice expressing APPsw

Cortex and hippocampus were taken from transgenic mice expressing APPsw (APP23) and wild-type mice at 6-months old. Total RNA was extracted and subjected to real-time RT-PCR using specific primers for each chaperone. Values were analysed and expressed as described in the legend for Figure 7(A). Results are means _ S.D. (*n* 3). ***, *P* 0.001; **, *P* 0.01; *, *P* 0.05.

the possible protective role of ER chaperones against A and AD. Therefore, we propose that non-toxic inducers of ER chaperones may be therapeutically beneficial for AD. It is well known that ER chaperones impair the aggregation of protein in the ER [19]. It has also been demonstrated that A aggregates intracellularly, and that this aggregation plays an important role in the pathogenesis of AD [49], although the precise location at which this aggregation occurs has not yet been determined. If that site is the ER, non-toxic inducers of ER chaperones may prove valuable in the treatment of AD, not only by decreasing the level of A , but also by impairing the aggregation of A in cells. Both previous studies [22] and the present one have examined the effect of ER chaperones on the level of A in APP-overexpressing cells. Similar analysis in wild-type cells may be important to estimate the role of ER chaperones in the production of A and the treatment of AD.

When we were preparing this manuscript, a related article was published by Kudo et al. [50], which showed that thapsigargin or tunicamycin, both of which induce ER chaperones, inhibit the maturation of APP and retained APP in the early compartment of the secretary pathway (such as the ER) when they decreased the amount of secreted A .

We thank Drs R. Austin (Pathology and Molecular Medicine, McMaster University, Ontario, Canada), D. Haslam (Department of Pediatrics, Washington University, St Louis, U.S.A.), K. Imaizumi (Division of Molecular and Cellular Biology, Miyazaki University, Miyazaki, Japan), R. de Crom (Cell Biology and Genetics, Erasmus University, Rotterdam, The Netherlands), M. Mori (Department of Molecular Genetics, Kumamoto University, Kumamoto, Japan), H. Kai (Graduate School of Medical and Pharmaceutical Sciences, Kumamoto University, Kumamoto, Japan), S. Ogawa (Department of Neuroanatomy, Kanazawa University, Ishikawa, Japan) and M. Staufenbiel (Nervous System Research Novartis Pharma Ltd., Basel, Switzerland) for the pcDNA3.1/GRP78, pCR3.1/ERdj3 pcDNA3.1/ERdj4 (ERdj4 J), pCD-X-h-gp96, pCR(HA), pCMVTag5A with Myc-taggec *CNX* gene, pCI-neo containing the *ORP150* gene plasmids and APP23 transgenic mice respectively. This work was supported by Grants-in-Aid for Scientific Research from the Ministry of Health, Labour, and Welfare of Japan, as well as by the Japan Science and Technology Agency, the Daiwa Securities Health Foundation, the Mochida Memorial Foundation for Medical and Pharmaceutical Research, the Suzuken Memorial Foundation and the Japan Research Foundation for Clinical Pharmacology.

REFERENCES

1 Hardy, J. and Selkoe, D. J. (2002) The amyloid hypothesis of Alzheimer's disease: progress and problems on the road to therapeutics. Science **297**, 353–356
2 Mattson, M. P. (2004) Pathways towards and away from Alzheimer's disease. Nature **430**, 631–639
3 Sisodia, S. S. and St. George-Hyslop, P. H. (2002) -Secretase, Notch, A and Alzheimer's disease: where do the presenilins fit in? Nat. Rev. Neurosci. **3**, 281–290
4 Selkoe, D. J. (1999) Translating cell biology into therapeutic advances in Alzheimer's disease. Nature **399**, A23–A31
5 Haass, C. (2004) Take five–BACE and the -secretase quartet conduct Alzheimer's amyloid -peptide generation. EMBO J. **23**, 483–488
6 Price, D. L., Sisodia, S. S. and Borchelt, D. R. (1998) Genetic neurodegenerative diseases: the human illness and transgenic models. Science **282**, 1079–1083
7 Mattson, M. P., Gary, D. S., Chan, S. L. and Duan, W. (2001) Perturbed endoplasmic reticulum function, synaptic apoptosis and the pathogenesis of Alzheimer's disease. Biochem. Soc. Symp. **67**, 151–162
8 Yan, S. D., Fu, J., Soto, C., Chen, X., Zhu, H., Al-Mohanna, F., Collison, K., Zhu, A., Stern, E., Saido, T. et al. (1997) An intracellular protein that binds amyloid- peptide and mediates neurotoxicity in Alzheimer's disease. Nature **389**, 689–695
9 Kaufman, R. J. (2002) Orchestrating the unfolded protein response in health and disease. J. Clin. Invest. **110**, 1389–1398
10 Ron, D. (2002) Translational control in the endoplasmic reticulum stress response. J. Clin. Invest. **110**, 1383–1388
11 Yoshida, H., Okada, T., Haze, K., Yanagi, H., Yura, T., Negishi, M. and Mori, K. (2000) ATF6 activated by proteolysis binds in the presence of NF-Y (CBF) directly to the *cis*-acting element responsible for the mammalian unfolded protein response. Mol. Cell Biol. **20**, 6755–6767
12 Luo, S., Baumeister, P., Yang, S., Abcouwer, S. F. and Lee, A. S. (2003) Induction of Grp78/BiP by translational block: activation of the Grp78 promoter by ATF4 through and upstream ATF/CRE site independent of the endoplasmic reticulum stress elements. J. Biol. Chem. **278**, 37375–37385
13 Harding, H. P., Novoa, I., Zhang, Y., Zeng, H., Wek, R., Schapira, M. and Ron, D. (2000) Regulated translation initiation controls stress-induced gene expression in mammalian cells. Mol. Cell **6**, 1099–1108
14 Katayama, T., Imaizumi, K., Honda, A., Yoneda, T., Kudo, T., Takeda, M., Mori, K., Rozmahel, R., Fraser, P., St. George-Hyslop, P. S. and Tohyama, M. (2001) Disturbed activation of endoplasmic reticulum stress transducers by familial Alzheimer's disease-linked presenilin-1 mutations. J. Biol. Chem. **276**, 43446–43454
15 Niwa, M., Sidrauski, C., Kaufman, R. J. and Walter, P. (1999) A role for presenilin-1 in nuclear accumulation of Ire1 fragments and induction of the mammalian unfolded protein response. Cell **99**, 691–702
16 Guo, Q., Fu, W., Sopher, B. L., Miller, M. W., Ware, C. B., Martin, G. M. and Mattson, M. P. (1999) Increased vulnerability of hippocampal neurons to excitotoxic necrosis in presenilin-1 mutant knock-in mice. Nat. Med. **5**, 101–106
17 Katayama, T., Imaizumi, K., Manabe, T., Hitomi, J., Kudo, T. and Tohyama, M. (2004) Induction of neuronal death by ER stress in Alzheimer's disease. J. Chem. Neuroanat. **28**, 67–78
18 Sato, N., Imaizumi, K., Manabe, T., Taniguchi, M., Hitomi, J., Katayama, T., Yoneda, T., Morihara, T., Yasuda, Y., Takagi, T. et al. (2001) Increased production of -amyloid and vulnerability to endoplasmic reticulum stress by an aberrant spliced form of presenilin 2. J. Biol. Chem. **276**, 2108–2114
19 Lee, A. S. (2001) The glucose-regulated proteins: stress induction and clinical applications. Trends. Biochem. Sci. **26**, 504–510
20 Tamatani, M., Matsuyama, T., Yamaguchi, A., Mitsuda, N., Tsukamoto, Y., Taniguchi, M., Che, Y. H., Ozawa, K., Hori, O., Nishimura, H. et al. (2001) ORP150 protects against hypoxia/ischemia-induced neuronal death. Nat. Med. **7**, 317–323
21 Ellgaard, L. and Helenius, A. (2001) ER quality control: towards an understanding at the molecular level. Curr. Opin. Cell Biol. **13**, 431–437
22 Yang, Y., Turner, R. S. and Gaut, J. R. (1998) The chaperone BiP/GRP78 binds to amyloid precursor protein and decreases A 40 and A 42 secretion. J. Biol. Chem. **273**, 25552–25555

23 Vattemi, G., Engel, W. K., McFerrin, J. and Askanas, V. (2004) Endoplasmic reticulum stress and unfolded protein response in inclusion body myositis muscle. Am. J. Pathol. **164**, 1–7
24 Kakimura, J., Kitamura, Y., Takata, K., Tsuchiya, D., Taniguchi, T., Gebicke-Haerter, P. J., Smith, M. A., Perry, G. and Shimohama, S. (2002) Possible involvement of ER chaperone Grp78 on reduced formation of amyloid- deposits. Ann. N.Y. Acad. Sci. **977**, 327–332
25 Hoozemans, J. J., Veerhuis, R., Van Haastert, E. S., Rozemuller, J. M., Baas, F., Eikelenboom, P. and Scheper, W. (2005) The unfolded protein response is activated in Alzheimer's disease. Acta Neuropathol. **110**, 165–172
26 Yoo, B. C., Kim, S. H., Cairns, N., Fountoulakis, M. and Lubec, G. (2001) Deranged expression of molecular chaperones in brains of patients with Alzheimer's disease. Biochem. Biophys. Res. Commun. **280**, 249–258
27 Takeda, K., Araki, W. and Tabira, T. (2004) Enhanced generation of intracellular A 42 amyloid peptide by mutation of presenilins PS1 and PS2. Eur. J. Neurosci. **19**, 258–264
28 Hoshino, T., Tsutsumi, S., Tomisato, W., Hwang, H. J., Tsuchiya, T. and Mizushima, T. (2003) Prostaglandin E2 protects gastric mucosal cells from apoptosis via EP2 and EP4 receptor activation. J. Biol. Chem. **278**, 12752–12758
29 Gu, Y., Misonou, H., Sato, T., Dohmae, N., Takio, K. and Ihara, Y. (2001) Distinct intramembrane cleavage of the -amyloid precursor protein family resembling -secretase-like cleavage of Notch. J. Biol. Chem. **276**, 35235–35238
30 Tomita, S., Kirino, Y. and Suzuki, T. (1998) A basic amino acid in the cytoplasmic domain of Alzheimer's -amyloid precursor protein (APP) is essential for cleavage of APP at the -site. J. Biol. Chem. **273**, 19304–19310
31 Taru, H. and Suzuki, T. (2004) Facilitation of stress-induced phosphorylation of -amyloid precursor protein family members by X11-like/Mint2 protein. J. Biol. Chem. **279**, 21628–21636
32 Forman, M. S., Cook, D. G., Leight, S., Doms, R. W. and Lee, V. M. (1997) Differential effects of the swedish mutant amyloid precursor protein on -amyloid accumulation and secretion in neurons and nonneuronal cells. J. Biol. Chem. **272**, 32247–32253
33 Landry, S. J. (2003) Structure and energetics of an allele-specific genetic interaction between dnaJ and dnaK: correlation of nuclear magnetic resonance chemical shift perturbations in the J-domain of Hsp40/DnaJ with binding affinity for the ATPase domain of Hsp70/DnaK. Biochemistry. **42**, 4926–4936
34 Yu, M., Haslam, R. H. and Haslam, D. B. (2000) HEDJ, an Hsp40 co-chaperone localized to the endoplasmic reticulum of human cells. J. Biol. Chem. **275**, 24984–24992
35 Shen, Y., Meunier, L. and Hendershot, L. M. (2002) Identification and characterization of a novel endoplasmic reticulum (ER) DnaJ homologue, which stimulates ATPase activity of BiP *in vitro* and is induced by ER stress. J. Biol. Chem. **277**, 15947–15956
36 Tomita, S., Kirino, Y. and Suzuki, T. (1998) Cleavage of Alzheimer's amyloid precursor protein (APP) by secretases occurs after *O*-glycosylation of APP in the protein secretory pathway. Identification of intracellular compartments in which APP cleavage occurs without using toxic agents that interfere with protein metabolism. J. Biol. Chem. **273**, 6277–6284
37 Stadelmann, C., Deckwerth, T. L., Srinivasan, A., Bancher, C., Bruck, W., Jellinger, K. and Lassmann, H. (1999) Activation of caspase-3 in single neurons and autophagic granules of granulovacuolar degeneration in Alzheimer's disease. Evidence for apoptotic cell death. Am. J. Pathol. **155**, 1459–1466
38 Games, D., Adams, D., Alessandrini, R., Barbour, R., Berthelette, P., Blackwell, C., Carr, T., Clemens, J., Donaldson, T., Gillespie, F. et al. (1995) Alzheimer-type neuropathology in transgenic mice overexpressing V717F -amyloid precursor protein. Nature **373**, 523–527
39 Sturchler-Pierrat, C., Abramowski, D., Duke, M., Wiederhold, K. H., Mistl, C., Rothacher, S., Ledermann, B., Burki, K., Frey, P., Paganetti, P. A. et al. (1997) Two amyloid precursor protein transgenic mouse models with Alzheimer disease-like pathology. Proc. Natl. Acad. Sci. U.S.A. **94**, 13287–13292
40 Van Dam, D., D'Hooge, R., Staufenbiel, M., Van Ginneken, C., Van Meir, F. and De Deyn, P. P. (2003) Age-dependent cognitive decline in the APP23 model precedes amyloid deposition. Eur. J. Neurosci. **17**, 388–396
41 Oda, Y., Hosokawa, N., Wada, I. and Nagata, K. (2003) EDEM as an acceptor of terminally misfolded glycoproteins released from calnexin. Science **299**, 1394–1397
42 Zhang, Y., McLaughlin, R., Goodyer, C. and LeBlanc, A. (2002) Selective cytotoxicity of intracellular amyloid peptide$_{1-42}$ through p53 and Bax in cultured primary human neurons. J. Cell. Biol. **156**, 519–529
43 Kadowaki, H., Nishitoh, H., Urano, F., Sadamitsu, C., Matsuzawa, A., Takeda, K., Masutani, H., Yodoi, J., Urano, Y., Nagano, T. and Ichijo, H. (2005) Amyloid induces neuronal cell death through ROS-mediated ASK1 activation. Cell Death Differ. **12**, 19–24
44 Wooden, S. K., Li, L. J., Navarro, D., Qadri, I., Pereira, L. and Lee, A. S. (1991) Transactivation of the *grp78* promoter by malfolded proteins, glycosylation block, and calcium ionophore is mediated through a proximal region containing a CCAAT motif which interacts with CTF/NF-I. Mol. Cell Biol. **11**, 5612–5623
45 Drummond, I. A., Lee, A. S., Resendez, Jr, E. and Steinhardt, R. A. (1987) Depletion of intracellular calcium stores by calcium ionophore A23187 induces the genes for glucose-regulated proteins in hamster fibroblasts. J. Biol. Chem. **262**, 12801–12805
46 Ferreiro, E., Oliveira, C. R. and Pereira, C. (2004) Involvement of endoplasmic reticulum Ca^2 release through ryanodine and inositol 1,4,5-triphosphate receptors in the neurotoxic effects induced by the amyloid- peptide. J. Neurosci. Res. **76**, 872–880
47 Demuro, A., Mina, E., Kayed, R., Milton, S. C., Parker, I. and Glabe, C. G. (2005) Calcium dysregulation and membrane disruption as a ubiquitous neurotoxic mechanism of soluble amyloid oligomers. J. Biol. Chem. **280**, 17294–17300
48 Cao, X. and Sudhof, T. C. (2001) A transcriptionally [correction of transcriptively] active complex of APP with Fe65 and histone acetyltransferase Tip60. Science **293**, 115–120
49 Hartmann, T. (1999) Intracellular biology of Alzheimer's disease amyloid peptide. Eur. Arch. Psychiatry Clin. Neurosci. **249**, 291–298
50 Kudo, T., Okumura, M., Imaizumi, K., Araki, W., Morihara, T., Tanimukai, H., Kamagata, E., Tabuchi, N., Kimura, R., Kanayama, D. et al. (2006) Altered localization of amyloid precursor protein under endoplasmic reticulum stress. Biochem. Biophys. Res. Commun. **344**, 525–530

Received 30 August 2006/24 November 2006; accepted 29 November 2006
Published as BJ Immediate Publication 29 November 2006, doi:10.1042/BJ20061318

0026-895X/07/7103-860–870$20.00
MOLECULAR PHARMACOLOGY

Mol Pharmacol 71:860–870, 2007

Vol. 71, No
27698/31821
Printed in U.S.

Up-Regulation of 150-kDa Oxygen-Regulated Protein by Celecoxib in Human Gastric Carcinoma Cells

Takushi Namba, Tatsuya Hoshino, Ken-ichiro Tanaka, Shinji Tsutsumi, Tomoaki Ishihara, Shinji Mima, Keitarou Suzuki, Satoshi Ogawa, and Tohru Mizushima

Graduate School of Medical and Pharmaceutical Sciences, Kumamoto University, Kumamoto, Japan (T.N., T.H., K.-i.T., S.T., T.I., S.M., K.S., T.M.); and Department of Neuroanatomy, Kanazawa University Medical School, Kanazawa, Japan (S.O.)

Received June 6, 2006; accepted December 12, 2006

ABSTRACT

Induction of apoptosis by nonsteroidal anti-inflammatory drugs, such as celecoxib, is involved in their antitumor activity. An endoplasmic reticulum chaperone, 150-kDa oxygen-regulated protein (ORP150) is essential for the maintenance of cellular viability under hypoxia and is reported to be overexpressed in clinically isolated tumors. We here found that ORP150 was up-regulated by celecoxib in human gastric carcinoma cells. In conjunction with the suppression of tumor growth, orally administered celecoxib up-regulated ORP150 in xenograft tumors. Both the ATF4 and ATF6 pathways were activated by celecoxib, and suppression of ATF4 and ATF6 mRNA expression by small interfering RNA (siRNA) inhibited the celecoxib-dependent up-regulation of ORP150. Celecoxib administration led to an increase in the intracellular concentration of Ca^2 , whereas 1,2-bis(2-aminophenoxy)ethane-*N,N,N ,N* -tetraacetic acid-acetoxymethyl ester, an intracellular Ca^2 chelator, inhibited the up-regulation of ORP150 and the activation of the ATF4 and ATF6 pathways. These results suggest that these Ca^2 -activated pathways are involved in the celecoxib-mediated up-regulation of ORP150. Clones overexpressing ORP150 were less susceptible to celecoxib-induced, but not staurosporine-induced, apoptosis and displayed less up-regulation of C/EBP homologous transcription factor (CHOP), a transcription factor with apoptosis-inducing activity. In contrast, siRNA for ORP150 stimulated apoptosis and expression of CHOP in the presence of celecoxib but not staurosporine. These results suggest that up-regulation of ORP150 in cancer cells inhibits celecoxib-induced apoptosis, thereby decreasing the potential antitumor activity of celecoxib.

Nonsteroidal anti-inflammatory drugs (NSAIDs) are made up of a useful family of therapeutics, accounting for nearly 5% of all prescribed medications (Smalley et al., 1995). In addition to their anti-inflammatory effects, recent epidemiological studies have revealed that prolonged NSAID use reduces the risk of cancer (such as colonic, rectal, and stomach cancer), and preclinical and clinical studies have indicated that some NSAIDs, in particular celecoxib, are effective in the treatment and prevention of cancer (Wang et al., 2003). The antitumor activity of NSAIDs involves various mechanisms, including cell growth suppression, inhibition of angiogenesis, and inhibition of metastasis. In particular, NSAID-induced apoptosis in cancer cells is thought to play an important role in the antitumor action of this class of drugs (Gupta and Dubois, 2001; Kismet et al., 2004).

Together with the anti-inflammatory action of NSAIDs, NSAID-induced apoptosis was only thought to be mediated through the NSAID-dependent inhibition of cyclooxygenase (COX), an enzyme essential for the synthesis of prostaglandins (PGs). This belief was based on the inhibition of cellular apoptosis by PGs, such as PGE_2, and the overexpression of COX-2 (a subtype of COX) in various types of clinically iso-

We thank to Dr. K. Kawahara (Kumamoto University) for helpful suggestions. This work was supported by grants-in-aid for scientific research from the Ministry of Health, Labor, and Welfare of Japan as well as by the Suzuken Memorial Foundation, the Tokyo Biochemical Research Foundation, Kumamoto Technology and Industry Foundation, and the Japan Research Foundation for Clinical Pharmacology.

Article, publication date, and citation information can be found at http://molpharm.aspetjournals.org.
doi:10.1124/mol.106.027698.

ABBREVIATIONS: NSAID, nonsteroidal anti-inflammatory drug; COX, cyclooxygenase; PG, prostaglandin; AGS, apoptosis in human gastric carcinoma; ER, endoplasmic reticulum; IRE1, protein-kinase and site-specific endoribonuclease; PERK, eukaryotic translation initiation factor 2 kinase; ATF, activating transcription factor; eIF2 , eukaryotic initiation factor-2 ; CHOP, C/EBP homologous transcription factor; ORP150, 150-kDa oxygen-regulated protein; GRP, glucose-regulated protein; AM, acetoxymethyl ester; BAPTA, 1,2-bis(2-aminophenoxy)ethane-*N,N,N ,N* -tetraacetic acid; PARP, poly(ADP-ribose)polymerase; siRNA, small interfering RNA; PCR, polymerase chain reaction; FITC, fluorescein isothiocyanate; FACS, fluorescence activated cell sorting; PI, propidium iodide; PIPES, piperazine-*N,N* -bis(2-ethanesulfonic acid); CHAPS, 3-[(3-cholamidopropyl)dimethylammonio]propanesulfonate; RT-PCR, reverse transcription-polymerase chain reaction; ERSE, endoplasmic reticulum stress response element; XBP-1, X box binding protein; ROSE, reactive oxygen species; VEGF, vascular endothelial growth factor.

lated tumors and cancer cell lines (Eberhart et al., 1994; Ristimaki et al., 1997). However, a derivative of the NSAID sulindac (sulindac sulfone), which has no COX-inhibitory activity, has subsequently been shown to induce apoptosis in tumor cells, whereas it has been demonstrated that some NSAIDs induce apoptosis in COX-null fibroblasts and in tumor cells without COX expression (Hanif et al., 1996; Elder et al., 1997; Zhang et al., 1999). Therefore, COX-independent mechanisms are also clearly involved in NSAID-induced apoptosis.

To investigate this COX-independent mechanism, we systematically searched for genes whose expression is up-regulated by NSAIDs in concert with induction of apoptosis in human gastric carcinoma (AGS) cells. This study revealed that various endoplasmic reticulum (ER) stress response-related genes are up-regulated by NSAIDs (Mima et al., 2005). The ER stress response is induced by accumulation of unfolded protein in the ER, a process involving three types of ER transmembrane proteins: protein-kinase and site-specific endoribonuclease (IRE1), protein kinase R-like ER kinase (PERK), and activating transcription factor (ATF) 6 (Yoshida et al., 2000; Kaufman, 2002; Ron, 2002). ER stressors phosphorylate PERK, which in turn phosphorylates eukaryotic initiation factor-2 (eIF2), leading to activation of ATF4 expression (ATF4 pathway) (Luo et al., 2003). ER stressors also cause cleavage of p90-ATF6 into p50-ATF6, which translocates to the nucleus (ATF6 pathway) (Yoshida et al., 2000). Both ATF4 and p50-ATF6 specifically activate transcription of ER stress response-related genes. ER stress response-related proteins contain not only ER chaperones (such as GRP78), which confer protection against stressors by refolding unfolded proteins in the ER, but also C/EBP homologous transcription factor (CHOP), a transcription factor with apoptosis-inducing activity (Zinszner et al., 1998). We have previously shown, using both CHOP-deficient mice and a dominant-negative form of CHOP, that this CHOP induction is important for NSAID-induced apoptosis (Tsutsumi et al., 2004). We have also recently reported that up-regulation of GRP78 by celecoxib protects cancer cells from celecoxib-induced apoptosis, decreasing the potential antitumor activity of the drug (Tsutsumi et al., 2006). Therefore, ER stress response seems to be important for elucidating the mechanism of NSAID-induced apoptosis.

Another ER chaperone, 150-kDa oxygen-regulated protein (ORP150), was originally identified in cultured astrocytes exposed to hypoxia (Kuwabara et al., 1996). Cellular expression of ORP150 confers resistance to apoptosis induced not only by hypoxia but also by glutamate and -amino-3-hydroxy-5-methylisoxazole-propionate (Ozawa et al., 1999; Kitao et al., 2001; Tamatani et al., 2001; Asahi et al., 2002). Previous studies have reported that ORP150 is up-regulated under various pathological conditions, and this up-regulation has been implicated in the progression of diabetes, atherosclerotic plaque, and ischemia in brain (Tsukamoto et al., 1996; Matsushita et al., 1998; Asahi et al., 2002; Ozawa et al., 2005). Furthermore, recent papers have described the up-regulation of ORP150 in clinically isolated tumors and cancer cell lines (Tsukamoto et al., 1998; Miyagi et al., 2002). However, being different from well studied ER chaperones, such as GRP78, the mechanism underlying the up-regulation of ORP150 remains unclear. In this study, we demonstrate that celecoxib up-regulates ORP150, and examine its action in AGS cells. Our findings suggest that up-regulation of ORP150 decreases the antitumor activity of the drug by inhibiting apoptosis. We also provide evidence that both the ATF4 and ATF6 pathways are involved in this celecoxib-induced up-regulation of ORP150.

Materials and Methods

Chemicals, Plasmids, and Animals. RPMI 1640 medium was obtained from Nissui (Tokyo, Japan). Fetal bovine serum was purchased from Gibco Co. (Carlsbad, CA). Pluronic F127, fluo-3/AM and BAPTA-AM were obtained from Dojindo Co. (Kumamoto, Japan). Staurosporine was purchased from Sigma-Aldrich (St. Louis, MO). Indomethacin was obtained from Wako Pure Chemicals (Tokyo, Japan). Celecoxib was from LKT Laboratories Inc. (St. Paul, MN). Antibodies against ATF4, ATF6, lamin, pro-caspase-3, and actin were purchased from Santa Cruz Biotechnology, Inc. (Santa Cruz, CA). An antibody against poly(ADP-ribose)polymerase (PARP) was from Cell Signaling Technology Inc. (Beverly, MA). An antibody against ORP150 came from our laboratory stock (Tsukamoto et al., 1998). The RNeasy kit, siRNAs, and HiPerFect and RNAiFect transfection reagent were from QIAGEN (Valencia, CA). Acetyl-DEVD-methylcoumarin amide was from Peptide Institute Inc. (Osaka, Japan). A first-strand cDNA synthesis kit was purchased from Amersham (Little Chalfont, Buckinghamshire, UK). Lipofectamine (TM2000) and pcDNA3.1 plasmid were obtained from Invitrogen. SYBR GREEN PCR Master Mix was from Applied Biosystems (Foster City, CA). Annexin V-FITC apoptosis detection kit I was from BD Biosciences (San Jose, CA). Female ICR nude mice (5 weeks of age) were obtained from the Kyudoh Co. (Saga, Japan). The experiments and procedures described here were carried out in accordance with the Guide for the Care and Use of Laboratory Animals as adopted and promulgated by the National Institutes of Health, and they were approved by the Animal Care Committee of Kumamoto University.

Cell Culture and Overexpression of ORP150. AGS, MKN45, and Kato III are human carcinoma cell lines derived from stomach. Cells were cultured in RPMI 1640 medium supplemented with 10% fetal bovine serum, 100 U/ml penicillin, and 100 g/ml streptomycin in a humidified atmosphere of 95% air with 5% CO_2 at 37°C. NSAIDs were dissolved in dimethyl sulfoxide, and control experiments were performed in the same concentrations of dimethyl sulfoxide alone. Cells were exposed to NSAIDs by changing the medium. Unless otherwise noted, cells (0.8 10^4 cells per well in 24-well plates, 4 10^4 cells per well in six-well plates, 6 10^5 cells in 100-mm plates) were cultured for 24 h before use in experiments. Transfection of AGS cells with plasmids (pCI-neo containing the *ORP150* gene) was carried out using Lipofectamine (TM2000) according to the manufacturer's protocols. The stable transfectants expressing ORP150 were selected by immunoblotting analysis. Positive clones were maintained in the presence of 800 g/ml Geneticin (G-418).

Annexin V binding by Fluorescence-Activated Cell Sorting. Experiments were done using Annexin V-FITC apoptosis detection kit I according to the manufacturer's protocols. Briefly, cells were gently washed with phosphate-buffered saline and the binding buffer and finally resuspended in the binding buffer. After addition of Annexin V-FITC and PI solutions, samples were incubated for 15 min at room temperature in the dark. Samples were scanned with a FACSCalibur (BD Biosciences) cell sorter and analyzed by CellQuest software (BD Biosciences). Plots in Annexin V-positive/PI-negative quadrant were counting as apoptotic cells.

Caspase Activity Assay. The caspase-3-like activity was determined as described previously (Hoshino et al., 2003). Briefly, cells were collected by centrifugation and suspended in extraction buffer (50 mM PIPES, pH 7.0, 50 mM KCl, 5 mM EGTA, 2 mM $MgCl_2$, and 1 mM dithiothreitol). Suspensions were sonicated and centrifuged, after which the supernatants were incubated with fluorogenic peptide substrates (acetyl-DEVD-methylcoumarin amide) in reaction

buffer (100 mM HEPES-KOH, pH 7.5, 10% sucrose, 0.1% CHAPS, and 1 mg/ml bovine serum albumin) for 15 min at 37°C. The release of aminomethylcoumarin was determined using a fluorescence spectrophotometer. One unit of protease activity was defined as the amount of enzyme required to release 1 pmol of aminomethylcoumarin per minute. For statistical analysis, we measured three different samples in the same experiment.

Real-Time Reverse Transcription-PCR Analysis. Total RNA was extracted from cells using an RNeasy kit according to the manufacturer's protocols. Samples were reverse-transcribed using a first-strand cDNA synthesis kit according to the manufacturer's instructions. Synthesized cDNA was applied to real-time RT-PCR (ABI Prism 7700) using SYBR GREEN PCR Master Mix and analyzed with ABI Prism 7700 Sequence Detection software according to the manufacturer's instructions. Real-time cycle conditions were 2 min at 50°C, followed by 10 min at 90°C, and finally 45 cycles each at 95°C for 30 s and 63°C for 60 s. Specificity was confirmed by electrophoretic analysis of the reaction products and by inclusion of template- or reverse transcriptase-free controls. To normalize the amount of total RNA present in each reaction, the actin gene was used as an internal standard. For statistical analysis, we performed PCR reaction three times on the same sample. Furthermore, we confirmed results by performing at least two independent experiments.

Primers were designed using the Primer3 Web site (http://frodo.wi.mit.edu/cgi-bin/primer3/primer3_www.cgi). Primers are listed as follows (name: forward primer and reverse primer): ATF4: 5 -tcaaacctcatgggttctcc-3 and 5 -gtgtcatccaacgtggtcag-3 ; ATF6: 5 -ctccgagatcagcagaggaa-3 and 5 -aatgactcagggatggtgct-3 ; CHOP: 5 -tgcctttctcttcggacact-3 and 5 -tgtgacctctgctggttctg-3 ; GRP78: 5 -tagcgtatggtgctgctgtc-3 and 5 -tttgtcaggggtctttcacc-3 ; ORP150: 5 -gaagatgcagagcccatttc-3 and 5 -tctgctccaggacctcctaa-3 ; GRP94: 5 -tggatcttgctgtggttttg-3 and 5 -tgaggcgaagcattctttct-3 ; calnexin: 5 -tgaagaagatggtggcactg-3 and 5 -cgtggctttctgtttcttgg-3 ; and calreticulin: 5 -tcaccaacgatgaggcatac-3 and 5 -tcctcgtcctgtttgtcctt-3 .

Northern Blotting. Total RNA was extracted by use of an RNeasy kit, according to the manufacturer's specifications. Samples were separated by agarose gel electrophoresis in the presence of 6.3% formaldehyde, and blotted onto nylon membranes (Amersham Bioscience). For obtaining RNA probe, PCR-amplified partial DNA fragments of *ORP150* (407 base pairs) were cloned into a pBluescript II SK ( ) vector (Stratagene, La Jolla, CA), and RNA probe was prepared using DIG Northern Starter kit (Roche Diagnostics, Indianapolis, IN). After hybridization and washing, membranes were analyzed with LAS 1000 plus (FUJIX Ltd., Kyoto, Japan).

Immunoblotting Analysis. Whole-cell and nuclear extracts were prepared as described previously (Tsutsumi et al., 2002). The protein concentration of samples was determined by the Bradford method (Bradford, 1976). Samples were applied to polyacrylamide SDS gels, subjected to electrophoresis, and the resultant proteins then immunoblotted with respective antibodies.

Xenograft Tumor Growth. The effect of celecoxib on xenograft tumor growth was examined as described previously (Tsutsumi et al., 2006). Briefly, each nude mouse was inoculated s.c. in the right hind footpad with 2 10^6 cells of MKN45. When tumors reached a mean volume of 66 14 mm^3, the mice began to receive a single daily oral dose of celecoxib in 1% methylcellulose, a protocol that continued for the duration of the study. Tumors were measured every 5 days, and their volumes were calculated. For examination of ORP150 expression in tumors, tumor xenografts (dissected into 1-mm pieces) were solubilized with buffer and subjected to immunoblotting analysis.

Measurement of Intracellular Ca^2 Levels. The intracellular Ca^2 levels were monitored as described previously (Tanaka et al., 2005). Cells were incubated with 4 M fluo-3/AM in assay buffer (115 mM NaCl, 5.4 mM KCl, 1.8 mM $CaCl_2$, 0.8 mM $MgCl_2$, 20 mM HEPES, 13.8 mM glucose, 0.1% bovine serum albumin, 0.04% Pluronic F127, and 2 mM probenecid) for 40 min at 37°C. After washing, cells were suspended in assay buffer, again containing 2 mM probenecid. Fluo-3 fluorescence of cells in a water-jacketed cuvette was measured with a Hitachi F-4500 spectrofluorophotometer. Maximum and minimum fluorescence values (F_{max} and F_{min}) were obtained by adding 10 M ionomycin and 10 M ionomycin plus 5 mM EGTA (in Ca^2 -free medium), respectively. The intracellular Ca^2 level was calculated according to the equation $[Ca^2]_i$ $K_d(F$ $F_{min})/(F_{max}$ $F)$, where K_d is the apparent dissociation constant (40 nM) of the fluorescent dye-Ca^2 complex. For statistical analysis, we measured three different samples in three independent experiments.

siRNA Targeting of Genes. We used siRNA of 5 -cagugauguu gaaggagaadTdT-3 and 5 -uucuccuucaacaucacugdTdT-3 , 5 -gccuaggucucuuagaugadTdT-3 and 5 -ucaucuaagagaccuaggcdTdT-3 or 5 .

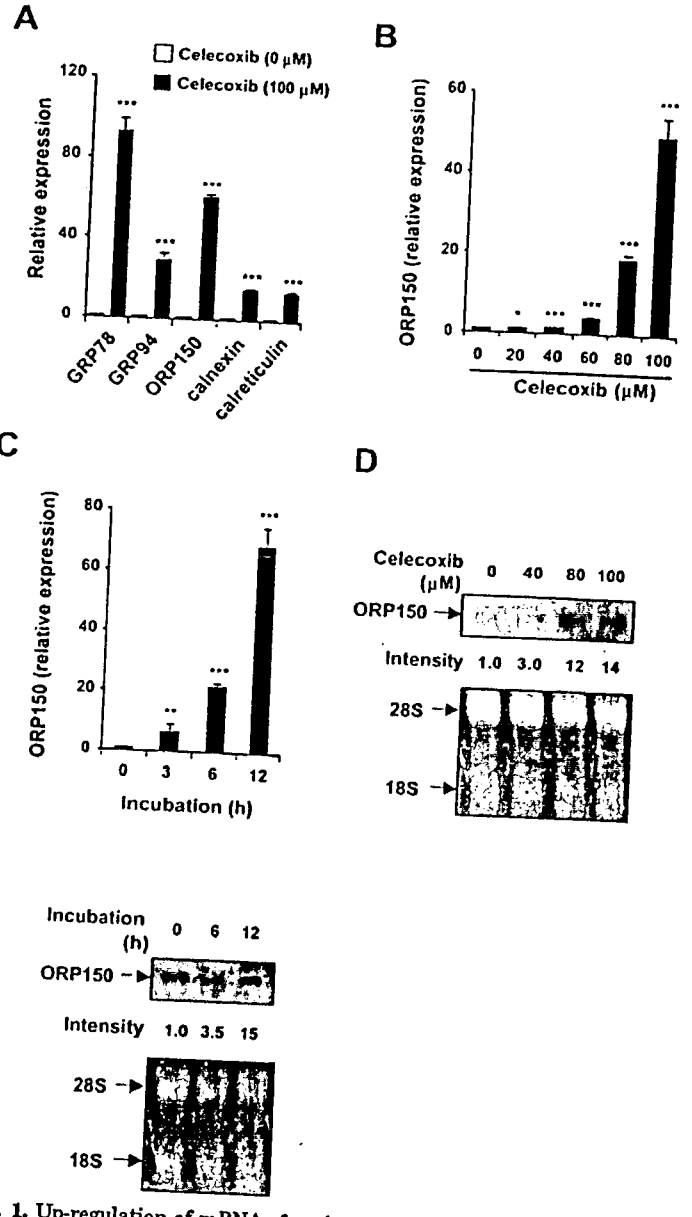

Fig. 1. Up-regulation of mRNA of various ER chaperone genes by celecoxib. AGS cells were incubated with either the indicated concentrations (A, B, and D) or 100 M of celecoxib (C and E) for 12 h (A, B, and D) or the time periods indicated (C and E) and total RNA extracted. Samples were subjected to real-time RT-PCR using a specific primer for each gene. Values were normalized to actin gene expression and expressed relative to the control sample (i.e., without celecoxib). Values are given as mean S.D. (n 3). , P 0.001; , P 0.01; , P 0.05 (A–C). Samples were also analyzed by Northern blotting analysis. Bottom panels show ribosomal RNA (18S and 28S) stained with ethidium bromide (D and E).

gcaaccaauuaucaguuuadTdT-3 and 5 -uaaacugauaauugguugcdTdT-3 as annealed oligonucleotides for repressing ORP150, ATF4, or ATF6 expression, respectively. AGS cells were transfected with siRNA using HiPerFect or RNAiFect transfection reagent according to the manufacturer's instructions. Nonsilencing siRNA (5 -uucuccgaacgugucacgudTdT-3 and 5 -acgugacacguucggagaadTdT-3) was used as a negative control.

Statistical Analysis. All values are expressed as the mean S.D. One-way analysis of variance followed by Scheffé's multiple comparison test was used for evaluation of differences between groups. The Student's t test for unpaired results was used for the evaluation of differences between two groups. Differences were considered to be significant for values of P 0.05.

Results

Celecoxib Up-Regulates Various ER Chaperones. In a previous report, we showed that NSAIDs (such as celecoxib, indomethacin, and diclofenac) up-regulate GRP78 expression in primary cultures of guinea pig gastric mucosal cells (Tsutsumi et al., 2004) and AGS cells (Tsutsumi et al., 2006). Here, we used real-time RT-PCR techniques to examine the effect of celecoxib on mRNA expression of various ER chaperone genes in AGS cells. As shown in Fig. 1A, celecoxib up-regulated GRP78 mRNA, as described previously (Tsutsumi et al., 2006). A similar result was obtained with all of the other ER chaperones tested, i.e., GRP94, ORP150, calnexin, and calreticulin (Fig. 1A). Of these, we focused on ORP150 in the following experiments. The dose-response and time-course properties of celecoxib-dependent up-regulation of ORP150 mRNA expression are shown in Fig. 1, B and C. Both reflect similar results to those obtained using GRP78 mRNA, as reported in our previous article (Tsutsumi et al., 2006). We also confirmed celecoxib-dependent up-regulation of ORP150 mRNA expression by Northern blotting analysis (Fig. 1, D and E).

Immunoblotting experiments revealed that celecoxib also up-regulates ORP150 at the protein level (Fig. 2A). A similar response was observed with another NSAID, indomethacin, suggesting that we were not observing a celecoxib-specific phenomenon.

COX exists as two subtypes, COX-1 and COX-2, for which celecoxib is COX-2-selective. We examined the celecoxib-dependent up-regulation of ORP150 in Kato III cells, in which COX-1 but not COX-2 mRNA is expressed (Saukkonen et al., 2001). This phenotype was confirmed by RT-PCR (data not shown). As shown in Fig. 2B, celecoxib up-regulated ORP150 even in Kato III cells; thus, a COX-2-selective NSAID up-regulated ORP150 in cells lacking COX-2 expression, suggesting that up-regulation of ORP150 by NSAIDs is independent of COX inhibition. For further confirmation of this point, we examined the effect of PGE_2 on the up-regulation of ORP150 and found that PGE_2 did not affect the expression of ORP150 in the presence or absence of celecoxib (data not shown).

We also examined the effect of celecoxib on ORP150 expression in tumors in vivo. Tumors were developed in nude mice by inoculation (s.c.) of MKN45 cells in which celecoxib-dependent up-regulation of ORP150 was confirmed in vitro (data not shown). Oral administration of celecoxib clearly inhibited the growth of xenograft tumors (Fig. 3C), this being consistent with our previous report (Tsutsumi et al., 2006).

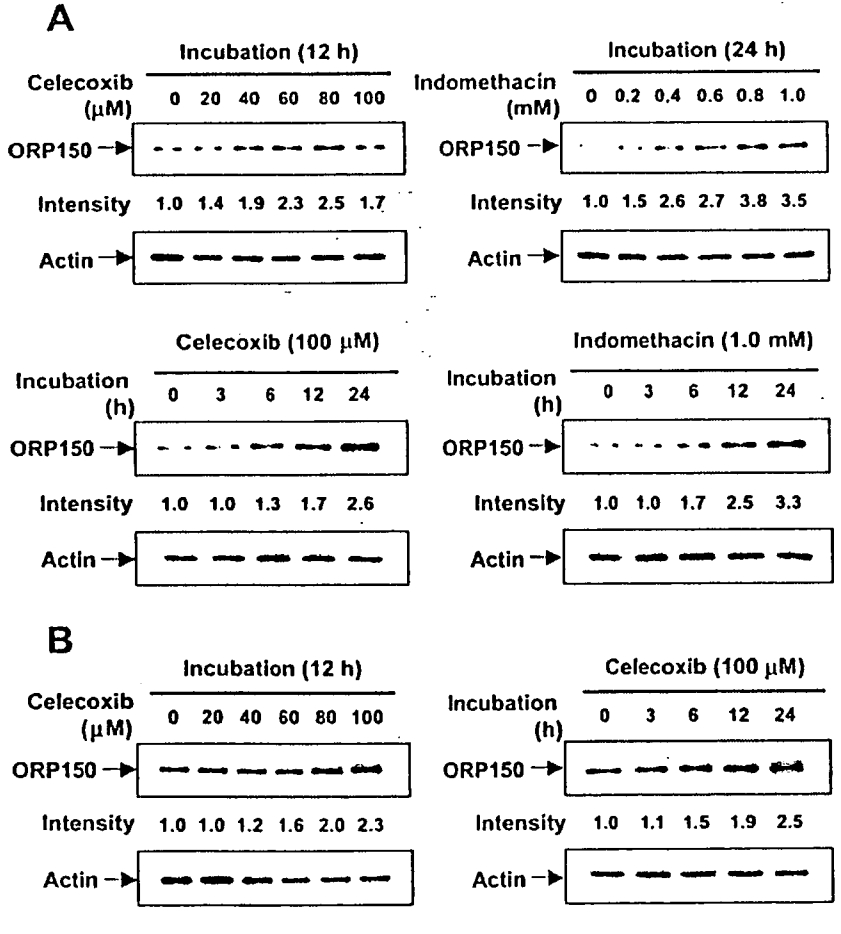

Fig. 2. Up-regulation of ORP150 by NSAIDs. AGS (A) or Kato III (B) cells were incubated with various concentrations of celecoxib or indomethacin for the indicated periods. Whole-cell extracts were analyzed by immunoblotting with an antibody against ORP150 or actin. The band intensity of ORP150 was determined by densitometric scanning. Gel-loading levels were compensated against the band intensity of actin and expressed relative to the control sample (i.e., without NSAIDs).

However, as shown in Fig. 3, A and B, the level of ORP150 in these tumors was also increased, indicating that celecoxib exerts this in vivo effect while simultaneously suppressing tumor growth.

Mechanism for Up-Regulation of ORP150 by Celecoxib. As outlined above, the mechanism underlying up-regulation of ORP150 by ER stressors is still unclear. Here, we used siRNA for ATF4 and ATF6 to examine the contribution of these transcription factors to celecoxib-dependent up-regulation of ORP150. As shown in Fig. 4, A and E, ATF4 mRNA and ATF4 protein was up-regulated by celecoxib as described previously (Tsutsumi et al., 2006), but, surprisingly, so, too, was ATF6 mRNA (Fig. 4B). The amount of p90 ATF6 or p50 ATF6 were decreased or increased, respectively, by celecoxib (Figs. 4E and 5F), suggesting that cleavage of p90-ATF6 into p50-ATF6 was stimulated by celecoxib as described previously (Tsutsumi et al., 2006). Transfection of a given siRNA decreased mRNA and protein levels of its target gene, but it had no effect on those of the other gene in both absence and presence of celecoxib (Fig. 4, A, B, and E). Furthermore, double transfection of siRNAs for both ATF4 and ATF6 resulted in suppression of mRNA levels of these genes to a similar extent to that seen with single transfection of each siRNA alone (Fig. 4, A and B). Celecoxib-dependent up-regulation of ORP150 mRNA was partially suppressed by siRNA for either ATF4 or ATF6 (Fig. 4C). However, interestingly, double transfection exerted a stronger suppressive effect than transfection of either siRNA alone (Fig. 4C). Similar results were obtained for celecoxib-dependent up-regulation of GRP78 mRNA (Fig. 4D). None of the transfections illustrated in Fig. 4 affected the baseline cell viability (data not shown). We also confirmed that both PERK and eIF2 were phosphorylated under the same conditions as in Fig. 4 (data

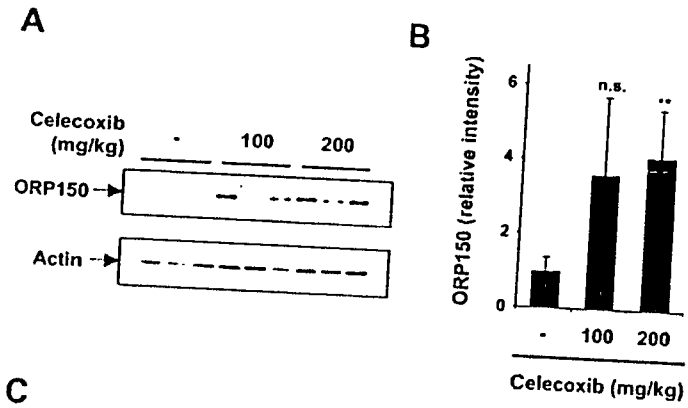

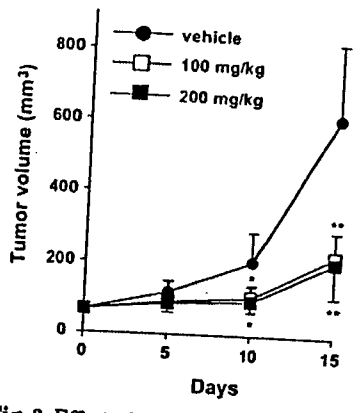

Fig. 3. Effect of celecoxib on growth of xenograft tumor and expression of ORP150 in nude mice. Each nude mouse (n 3) was inoculated s.c. with MKN45 cells, leading to tumor development. Celecoxib was then administered as a single daily oral dose for the duration of the study. Four days after celecoxib administration commenced, cell lysates prepared from tumors were analyzed by immunoblotting as described in the legend of Fig. 2 (A and B). Tumors were measured every 5 days and their volumes calculated (C). Values given are mean S.D. (n 5). , P 0.01; , P 0.05 (B and C).

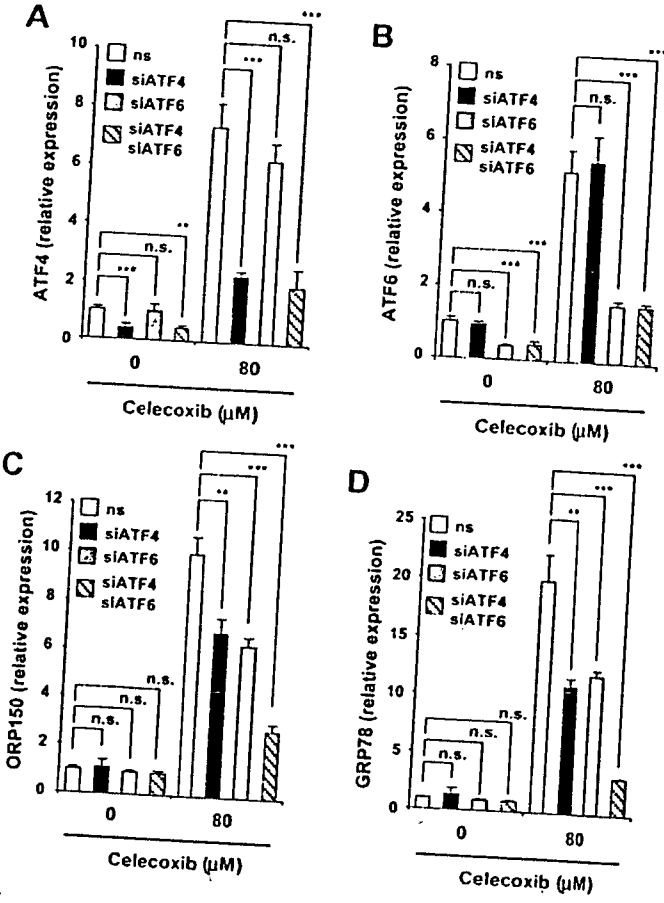

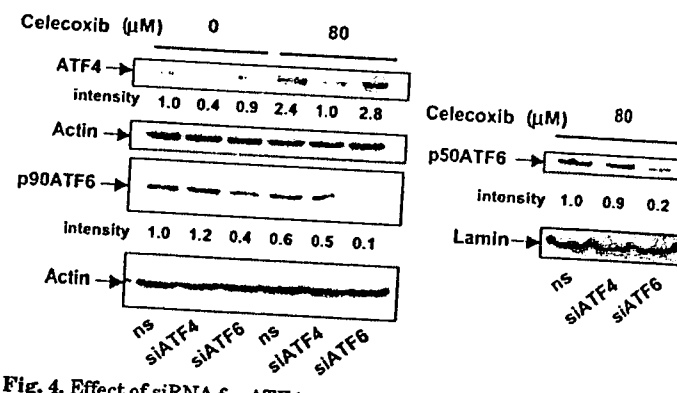

Fig. 4. Effect of siRNA for ATF4 and/or ATF6 on the celecoxib-dependent up-regulation of ORP150. AGS cells transfected with siRNA for ATF4 (siATF4), ATF6 (siATF6), and/or nonsilencing (ns) siRNA (the total amount of siRNA is fixed at 10 g) were incubated with or without 80 M celecoxib for 6 h. Total RNA was extracted and subjected to real-time RT-PCR by use of a specific primer for *ATF4* (A), *ATF6* (B), *ORP150* (C), and *GRP78* (D). Values were analyzed and expressed as described in the legend of Fig. 1. Values are shown as mean S.D. (n 3). , P 0.001; , P 0.01. E, whole-cell extracts (for ATF4, actin, and p90-ATF6) or nuclear extracts (for p50-ATF6 and lamin) were analyzed by immunoblotting as described in the legend to Fig. 2.

not shown). These results suggest that both the PERK-eIF2 -ATF4 and the ATF6 pathways are involved in the up-regulation of ORP150 by celecoxib.

We have previously reported that NSAIDs increase intracellular Ca^2 concentrations, leading us to suggest that this increase is involved in the NSAID-induced ER stress response (Tomisato et al., 2004; Tanaka et al., 2005; Tsutsumi et al., 2006). Here, we tested whether an increase in intracellular Ca^2 is involved in the celecoxib-dependent up-regulation of ORP150. First, we confirmed that celecoxib increases intracellular Ca^2 in a dose-dependent manner in AGS cells (Fig. 5A), this increase being consistent with our previous results (Tsutsumi et al., 2006). BAPTA-AM, an intracellular Ca^2 chelator, partially inhibited the celecoxib-dependent up-regulation of ORP150, GRP78, ATF4, and ATF6 mRNA and the cleavage of p90-ATF6 into p50-ATF6 (Fig. 5, B–F). At the concentrations used, BAPTA-AM did not affect cell viability (data not shown). These results suggest that an increase in intracellular Ca^2 is involved in the up-regulation of ORP150 through activation of both the ATF4 and ATF6 pathways.

Role of Up-Regulation of ORP150 in the in Vitro Antitumor Activity of Celecoxib. As described above, various mechanisms have been proposed for the chemopreventive and chemotherapeutic action of NSAIDs; these include inhibition of cell growth and stimulation of apoptosis. Here, we examined the role of celecoxib-dependent up-regulation of ORP150 in the antitumor activity of the drug in vitro. This was achieved by constructing stable transfectants of AGS cells that continuously overexpressed ORP150 (clones 3 and 5) (Fig. 6, A and B).

Figure 6C shows the cell growth curve for each clone; these curves were indistinguishable from that of the mock transfectant control. Therefore, up-regulation of ORP150 by celecoxib does not seem to be involved in its inhibition of cell growth.

We recently reported that celecoxib induces apoptosis but that up-regulation of GRP78 contributes to suppression of this apoptosis in AGS cells (Tsutsumi et al., 2006). We therefore examined the role of up-regulation of ORP150 in apoptosis using ORP150-overexpressing clones and siRNA for ORP150. Figure 6D shows the time course of celecoxib-dependent induction of apoptosis. Significant apoptosis was observed 3 h after the addition of celecoxib. Since treatment of cells with 80 M celecoxib for more than 12 h caused lower recovery of mRNA and protein (data not shown), we choose 6 h as a condition for observing celecoxib-dependent apoptosis. We examined the role of up-regulation of ORP150 in apoptosis by FACS analysis (counting annexin V-positive/PI-negative cells). As shown in Fig. 6, E and F, apoptotic cells (annexin V-positive/PI-negative cells) increased after the treatment of cells with celecoxib, and this increase was partially inhibited in ORP150-overexpressing clones. We also examined the effect of ORP150 overexpression on celecoxib-induced apoptosis by measuring caspase-3-like activity using fluorogenic peptide substrates and by monitoring cleavage of pro-caspase-3 and cleavage of PARP (a substrate of caspase-3) and obtained results similar to those from FACS analysis (Fig. 6, G and H). Furthermore, compared with the mock transfectant control, up-regulation of CHOP mRNA by celecoxib was partially suppressed in ORP150-overexpressing clones (Fig. 6I), suggesting that overexpression of ORP150 protects AGS cells from apoptosis through inhibition of *CHOP* expression. To examine the specificity of this antiapoptotic effect of ORP150, the apoptosis induced by staurosporine, a chemotherapy drug that lacks any ER stress response-inducing ability, was compared between ORP150-overexpressing clones and the mock transfectant control. As shown in Fig. 6K, staurosporine did not up-regulate ORP150

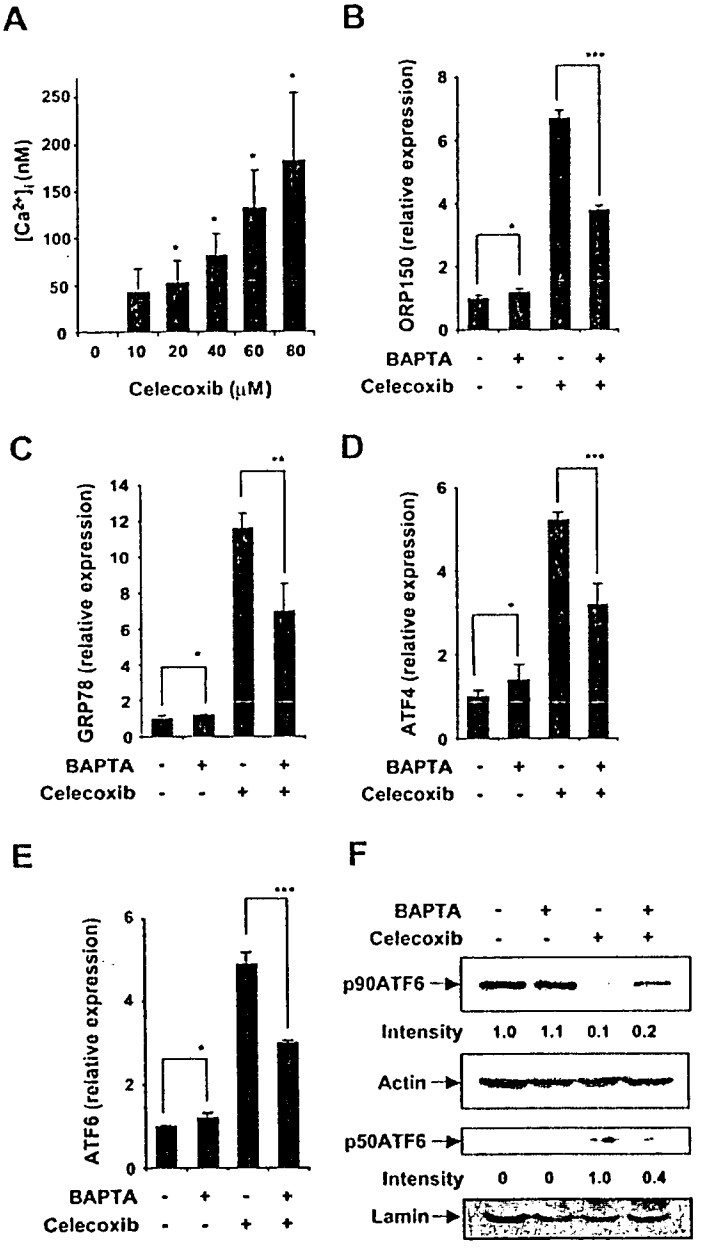

Fig. 5. Changes in intracellular Ca^2 concentration and its role in the celecoxib-dependent up-regulation of ORP150. The intracellular Ca^2 concentration was monitored using a fluo-3/AM assay system. The indicated concentrations of celecoxib were added to fluo-3/AM-loaded cells, and the time course of fluo-3 fluorescence change was monitored. The maximum value for the increase in the intracellular Ca^2 level ($[Ca^2]_i$) is shown (A). AGS cells were preincubated with or without 2 M BAPTA-AM for 1 h and further incubated with or without 80 M celecoxib in the presence or absence of 2 M BAPTA-AM for 6 h (B–F). The levels of ORP150 mRNA (B), GRP78 mRNA (C), ATF4 mRNA (D), ATF6 mRNA (E), and p50- and p90-ATF6 protein (F) were estimated by real-time RT-PCR or immunoblotting experiments as described in the legends of Figs. 1 and 4. Values are shown as mean S.D. (n 3). , P 0.001; , P 0.01; , P 0.05 (A–E).

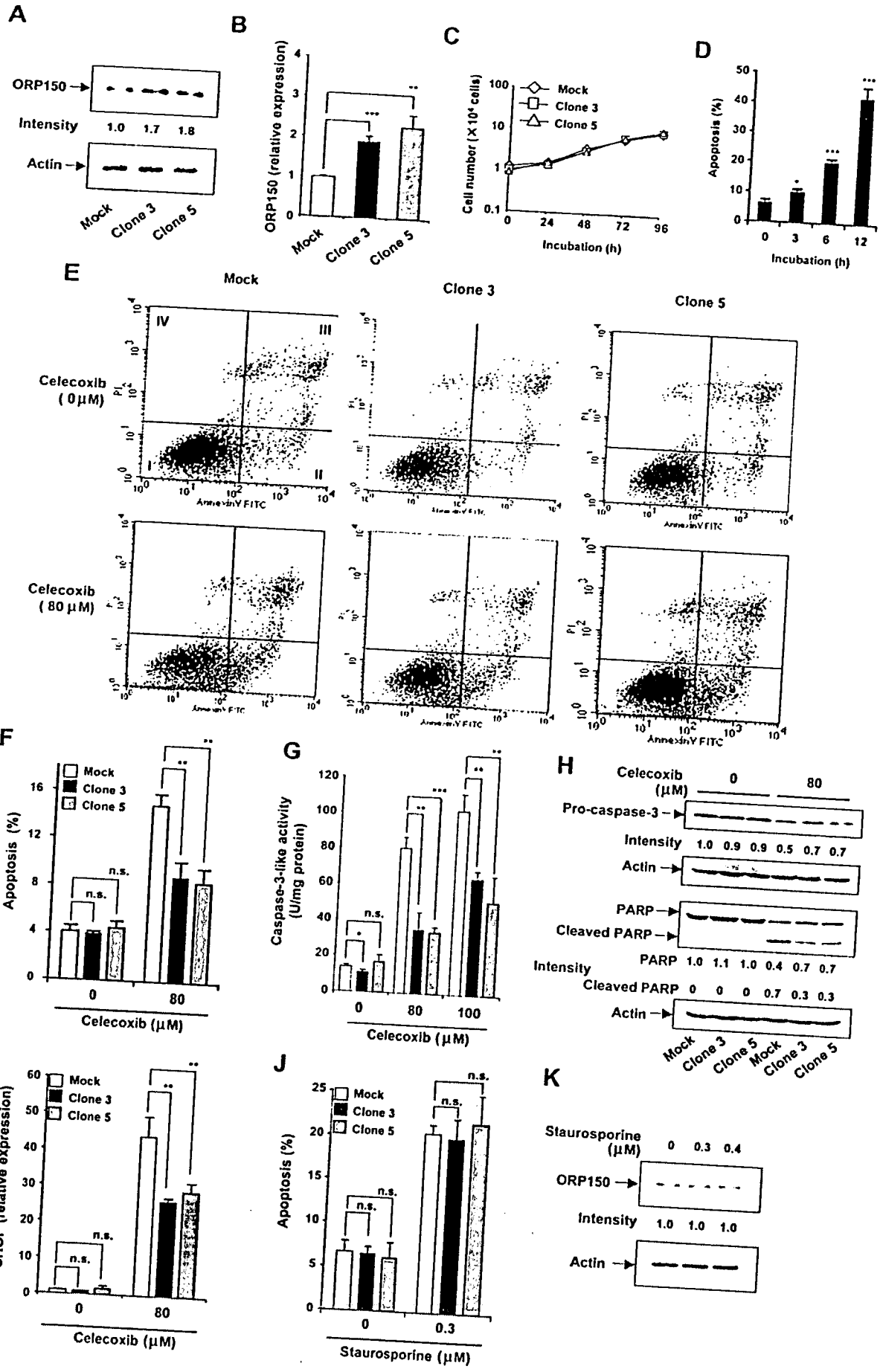
A
ORP150
Intensity 1.0 1.7 1.8
Actin
Mock
Clone 3
Clone 5
B
ORP150 (relative expression)
C
Cell number (X 10⁴ cells)
Mock
Clone 3
Clone 5
Incubation (h)
D
Apoptosis (%)
Incubation (h)
E
Mock
Clone 3
Clone 5
Celecoxib (0μM)
Celecoxib (80μM)
Annexin V FITC
F
Apoptosis (%)
n.s.
Celecoxib (μM)
G
Caspase-3-like activity (U/mg protein)
Celecoxib (μM)
H
Celecoxib (μM) 0 80
Pro-caspase-3
Intensity 1.0 0.9 0.9 0.5 0.7 0.7
Actin
PARP
Cleaved PARP
PARP 1.0 1.1 1.0 0.4 0.7 0.7
Intensity
Cleaved PARP 0 0 0 0.7 0.3 0.3
Actin
Mock Clone 3 Clone 5 Mock Clone 3 Clone 5
I
CHOP (relative expression)
Celecoxib (μM)
J
Apoptosis (%)
Staurosporine (μM)
K
Staurosporine (μM) 0 0.3 0.4
ORP150
Intensity 1.0 1.0 1.0
Actin

at concentrations that were sufficient to induce apoptosis (Fig. 6J), and there was no difference in the level of staurosporine-induced apoptosis between ORP150-overexpressing clones and the mock transfectant control (Fig. 6J). These results suggest that the suppression of apoptosis by overexpression of ORP150 is specific for apoptosis induced by chemotherapy drugs that induce an ER stress response.

Transfection of siRNA for ORP150 decreased the expression of ORP150 protein (Fig. 7A) and ORP150 mRNA (Fig. 7B) in the presence or absence of celecoxib. FACS analysis and analysis on caspase-3 showed that this transfection stimulated celecoxib-induced apoptosis (Fig. 7, C–F). Furthermore, this transfection stimulated celecoxib-induced CHOP mRNA expression (Fig. 7G). Together, these results support the idea that celecoxib-induced up-regulation of ORP150 protects cells from apoptosis induced by the drug. In contrast, as illustrated in Fig. 7H, transfection of siRNA for ORP150 had no effect on apoptosis induced by staurosporine, further supporting the idea that the antiapoptotic effect of ORP150 is specific for chemotherapy drugs that induce an ER stress response.

We also examined the effect of siRNA for ORP150 on celecoxib-dependent cell growth inhibition. Since the growth inhibition was observed with lower concentrations of celecoxib than apoptosis induction, we used 40 M celecoxib for this experiment. We confirmed that siRNA for ORP150 but not nonspecific siRNA suppressed the 40 M celecoxib-dependent induction of ORP150 mRNA (Fig. 7I). As shown in Fig. 7J, the growth of cells transfected with siRNA for ORP150 in the presence of celecoxib was slower than that with nonspecific siRNA. In contrast, there was no clear difference in cell growth between siRNA for ORP150 and nonspecific siRNA in the absence of celecoxib (Fig. 7J). These results suggest that celecoxib-induced up-regulation of ORP150 protects cells not only from apoptosis but also from growth inhibition induced by the drug.

Discussion

In this study, we have shown that celecoxib up-regulates ORP150 not only in cultured human gastric carcinoma cells but also in xenograft tumors in nude mice. Given that celecoxib (a COX-2-selective NSAID) up-regulated ORP150 in cells lacking COX-2 expression (Kato III cells) and that endogenously added PGE_2 did not affect this up-regulation, the up-regulation of ORP150 by celecoxib seems to occur independently of COX inhibition, as does the up-regulation of GRP78 by the same drug (Tsutsumi et al., 2006).

Although various ER stressors have been reported to up-regulate ORP150, the underlying molecular mechanism has remained unclear. As far as we are aware, the only available information is that the promoter of the *ORP150* gene contains an ER stress response element (ERSE) to which p50-ATF6 specifically binds, activating transcription (Kaneda et al., 2000). In this study, we investigated the molecular mechanism responsible for celecoxib-dependent up-regulation of ORP150 using an siRNA technique. siRNA for either ATF4 or ATF6 partially suppressed celecoxib-dependent up-regulation of ORP150, whereas double transfection of the two together proved even more inhibitory. We have previously reported that celecoxib causes sequential activation of PERK, eIF2 , and ATF4 in AGS cells (Tsutsumi et al., 2006). Furthermore, we showed that p90-ATF6 (the inactive form of ATF6 for ERSE-dependent transcription) is cleaved into p50-ATF6 (the active form) in the presence of celecoxib. Together, these results suggest that both the PERK-eIF2˜-ATF4 and the ATF6 pathways are involved in the celecoxib-dependent up-regulation of ORP150, this being consistent with up-regulation of GRP78 by other ER stressors (Yoshida et al., 2000; Luo et al., 2003). However, unlike other ER stressors (Yoshida et al., 2000), celecoxib also up-regulates the expression of ATF6 mRNA. At present, the underlying mechanism and its contribution to celecoxib-induced up-regulation of ORP150 remain unclear. Another ER transmembrane protein, IRE1, may also be involved in the celecoxib-induced up-regulation of ORP150. IRE1 splices the mRNA of X box binding protein 1 (XBP-1), thereby converting it into a potent activator of transcription from ERSE (Kaufman, 2002). We have previously reported that exposure to the NSAID indomethacin decreases the unspliced (inactive) and increases spliced (active) forms of the XBP-1 protein, respectively (Tsutsumi et al., 2004). However, since none of the *IRE1* or *XBP-1* siRNAs tested here significantly suppressed the target gene (data not shown), we could not test the contribution of the IRE1-XBP-1 pathway to celecoxib-induced up-regulation of ORP150.

In terms of the mechanism upstream of activation of ER transmembrane proteins by celecoxib, we propose that an increase in the intracellular Ca^2 concentration plays an important role. It is well known that an increase in intracellular Ca^2 induces the ER stress response (Drummond et al., 1987; Wooden et al., 1991). Here, we showed that celecoxib administration leads to a rise in the concentration of intracellular Ca^2 , whereas the application of the intracellular Ca^2 chelator, BAPTA-AM, inhibits the celecoxib-dependent up-regulation of ORP150 mRNA. In a recent study, we also demonstrated that all of the NSAIDs tested could cause membrane permeabilization and the increase in the intracellular Ca^2 level induced by celecoxib was inhibited under Ca^2 -free conditions (Tanaka et al., 2005), suggesting that stimulation of the influx of extracellular Ca^2 by permeabilization of cytoplasmic membranes is responsible for the observed NSAID-induced rise in intracellular Ca^2 . Celecoxib-dependent inhibition of sarcoplasmic/endoplasmic reticulum Ca^2 ATPase (an ER-located Ca^2 pump that is responsible

Fig. 6. Effect of overexpression of ORP150 on cell growth and apoptosis in AGS cells. The extent of expression of ORP150 in each clone (stable transfectant of ORP150 expression plasmid) or staurosporine-treated (6 h) AGS cells was estimated by immunoblotting experiments (A and K) or real-time RT-PCR (B) as described in the legend of Figs. 1 and 2. Cells from each clone were cultured for the indicated periods, and cell numbers were determined by direct cell counting (C). AGS cells were treated with 80 M celecoxib for indicated periods (D). Cells from each clone were cultured in the presence of the indicated concentrations of celecoxib (E–I) or staurosporine (J) for 6 h (E–H and J) or 3 h (I), and apoptotic cell numbers were determined by FACS (Annexin V-FITC and PI double staining) (D, E, F, and J). Caspase-3-like activities were measured (G). Total protein or RNA was extracted and subjected to immunoblotting with antibodies against pro-caspase-3 and PARP or real-time RT-PCR using a specific primer for CHOP, respectively (H and I). Values are given as mean S.E.M. (n 3). , P 0.001; , P 0.01; , P 0.05. One datum based on which we draw the F is shown (E). Cells contained in the quadrant of Annexin V-positive and PI-negative (shown as II in control sample in E) are counted as apoptotic cells (E and F).